Available online at www.sciencedirect.com
ScienceDirect
Deep-Sea Research II 55 (2008) 801–819
DEEP-SEA RESEARCH PART II
www.elsevier.com/locate/dsr2

Impact of iron on silicon utilization by diatoms in the Southern Ocean: A case study of Si/N cycle decoupling in a naturally iron-enriched area

Julie Mosseri, Bernard Quéguiner*, Leanne Armand, Véronique Cornet-Barthaux

Laboratoire d'Océanographie et de Biogéochimie, LOB-UMR 6535, OSU/Centre d'Océanologie de Marseille, Parc Scientifique et Technologique de Luminy, CNRS, Aix-Marseille Université, Case 901, F-13288 Marseille Cedex 09, France

Accepted 12 December 2007
Available online 11 April 2008

Abstract

Biogenic silica stocks and fluxes were investigated in austral summer over the naturally iron-fertilized Kerguelen Plateau and in nearby high-nutrient, low-chlorophyll (HNLC) off-plateau surface waters. The Kerguelen Plateau hosted a large-diatom bloom, with high levels of biogenic silica (BSi) but relatively low silicic acid ($Si(OH)_4$) uptake rates ($1100 \pm 600\,mmol\,m^{-2}$ and $8 \pm 4\,mmol\,m^{-2}\,d^{-1}$, respectively). Diatoms of the naturally iron-enriched area presented high affinities for silicic acid, allowing them in combination with a beneficial nutrient vertical supply to grow in low silicic acid waters ($<2\,\mu M$). $Si(OH)_4$ acid uptake rates were also compared with carbon and nitrogen uptake rates. As expected for diatoms growing in favourable nutrient conditions, and from previous artificial iron-enrichment experiments, Si:C and $Si:NO_3$ elemental uptake ratios of the natural diatom community of the plateau were close to 0.13 and 1, respectively. In contrast, diatom communities in the HNLC waters were composed of strongly silicified (high Si:C, $Si:NO_3$ uptake ratios) diatoms with low affinities for $Si(OH)_4$. Although the $Si:NO_3$ uptake ratio in the surface waters of the plateau was close to 1, the apparent consumption of nitrate on a seasonal basis was much lower ($\sim 5\,\mu M$) than the apparent consumption of silicic acid ($\sim 15\,\mu M$). This was mainly due to diatoms growing actively on ammonium (i.e. 39–77% of the total nitrogen uptake) produced by an intense heterotrophic activity. Thus we find that while Fe fertilization does increase N uptake with respect to Si uptake, rapid recycling of N decouples nitrogen and carbon export from silica export so that the "silicate pump" remains more efficient than that of N (or P). For this reason an iron-fertilized Southern Ocean is unlikely to experience nitrate exhaustion or export silicic acid to the global ocean.

Keywords: Silicon; Iron fertilization; Biogenic silica; Diatoms; Limiting factors

1. Introduction

Since the "Iron Hypothesis" (Martin, 1990) was proposed to solve the paradox of the "high-nutrient, low-chlorophyll" (HNLC) systems (Minas et al., 1986), numerous studies have investigated the impact of iron on phytoplankton growth and biogeochemical processes in HNLC areas (i.e. Southern Ocean, Equatorial Pacific, Subarctic Pacific). These studies were mainly conducted as bottle-enrichment experiments (e.g., Boyd et al., 1996) or as *in situ* mesoscale fertilizations (Boyd et al., 2000; see also review of De Baar et al., 2005). All of these experiments demonstrated that iron availability limited phytoplankton development and the corresponding use of macronutrients. The addition of iron (Fe) clearly stimulated phytoplankton growth, especially microphytoplankton groups such as diatoms, which typically presented the largest response to iron enrichment.

As the cell wall of diatoms is composed of biogenic silica (BSi), the growth of these algae is also strongly dependent on silicic acid ($Si(OH)_4$) availability. $Si(OH)_4$ uptake by diatoms is classically controlled by $Si(OH)_4$ external concentrations resulting in an hyperbolic uptake following Michaelis-Menten saturation functions. Other controlling factors have been identified including trace-metals (e.g., iron, zinc), floristic compositions, and complex interactions between the ability of diatoms to adjust their uptake and extent of silicification to environmental conditions (Martin-Jézéquel et al., 2000; Ragueneau et al., 2000). It turns out that in vast regions of HNLC systems, redefined as "high

*Corresponding author. Tel.: +33 4 91 82 9060; fax: +33 4 91 82 19 91.
E-mail address: bernard.queguiner@univmed.fr (B. Quéguiner).

0967-0645/$ - see front matter © 2008 Elsevier Ltd. All rights reserved.
doi:10.1016/j.dsr2.2007.12.003

nitrate, low-silicate, low-chlorophyll" waters or "HNLSLC" regions (Dugdale et al., 1995), diatom productivity may be controlled by both Fe and $Si(OH)_4$ availability. Both nutrients could be co-limiting in these areas, with the availability of Fe controlling the potential use of $Si(OH)_4$. In HNLSLC regions bottle incubation experiments have often shown that phytoplankton growth was stimulated in treatments with Fe addition only, and in most cases to a much greater degree in treatments with both Fe and $Si(OH)_4$ added together, whereas growth was not stimulated in treatments with only $Si(OH)_4$ addition (Coale et al., 1996; Boyd et al., 1999; Hutchins et al., 2001; Sedwick et al., 2002).

Early bottle iron-addition experiments showed that natural diatom communities under conditions of severe (<0.1 nM) Fe limitation exhibit high ratios of silicon to other elements (C, N) (Hutchins and Bruland, 1998; Takeda, 1998). Fe availability influences both $Si(OH)_4$ and NO_3^- uptake processes as well as Si:C and Si:N uptake ratios, although the exact mechanisms remain a matter of debate. With regard to $Si(OH)_4$ uptake processes, some studies have reported changes exclusively in the maximal specific Si uptake rate V_{max} (Hutchins et al., 1999; De La Rocha et al., 2000) or in the half-saturation constant for Si uptake rate K_S (Quéguiner, 2001) under iron-limiting conditions. Recent studies conducted in culture (Leynaert et al., 2004) or from *in situ* artificially Fe-enriched waters (Brzezinski et al., 2005) showed that both parameters could be affected by Fe availability, but not necessarily in the same direction.

Fe availability and its influence on phytoplankton community structure and nutrient cycling could have a large impact on the global carbon cycle, as already suggested by the "Iron Hypothesis" (Martin, 1990). Martin (1990) hypothesized that an increased organic carbon export due to a higher Fe supply from atmospheric dust deposition could explain the lower atmospheric concentrations of CO_2 during the glacial stages. Early observations from sedimentary records have supported this idea (Kumar et al., 1995), but more recent reviews have not found conclusive evidence (e.g., Sigman and Boyle, 2000).

One could expect that Fe fertilization, by boosting large diatoms that are considered the main drivers of the carbon biological pump (Buesseler, 1998), would favour the pumping and sequestration of carbon. By contrast, with high ratios of Si to other elements resulting from iron-depleted conditions, iron-limited areas would be rather more efficient in driving the "silicate pump" as defined by Dugdale et al. (1995). In the Southern Ocean the "silicate pump" runs at close to maximal efficiency in the modern ocean, i.e. little silicic acid remains in waters that leave the Southern Ocean (Dugdale et al., 1995; Trull et al., 2001). Thus for iron stimulation of diatoms to increase the carbon pump, iron must increase the uptake and export of carbon and other nutrients, as well as silica. However, *in situ* mesoscale Fe enrichments, despite stimulation of diatoms, have failed so far to demonstrate such an iron-related consistent stimulation of carbon export: the increase of carbon export due to Fe supply was null or low as compared to natural blooms or to the magnitude of primary production (Charette and Buesseler, 2000; Nodder et al., 2001; Boyd et al., 2004; Buesseler et al., 2005).

Although providing insights into how Fe availability could impact $Si(OH)_4$ uptake and ratios of Si to other elements, these latter experiments could have suffered from experimental artifacts due to the sudden perturbation of the environment and the short duration of the surveys as compared to the expected lag between production and vertical export. The examination of the present state-of-the-art of the Fe hypothesis thus clearly calls for new observations on unperturbed natural communities.

The KErguelen Ocean and Plateau compared Study (KEOPS) programme was conducted to investigate a naturally iron-fertilized area located in the core of the Southern Ocean, which is considered as the largest HNLC area and where the suppression of Fe limitation could potentially affect the carbon biological pump (Blain et al., 2007). The study area is located to the south-east of the Kerguelen Islands in the Indian sector of the Southern Ocean where a well-developed bloom is observed annually in satellite chlorophyll images. Over the Kerguelen Plateau upward iron transfer from deep iron-rich waters to the surface layer occurs through enhanced vertical mixing due to internal wave activities, originating mainly from internal tides (Park et al., 2008). In addition to a two-fold larger iron winter stock from wintertime deep convective mixing, the upward supply of iron to the surface waters over the Kerguelen plateau was estimated to be as high as $31\,nmol\,m^{-2}\,d^{-1}$ versus $4\,nmol\,m^{-2}\,d^{-1}$ in the surrounding HNLC waters (Blain et al., 2007). The objective of the KEOPS program is an impact study of this natural iron-fertilization process on the carbon biological pump and the cycling of climate-relevant chemical compounds. For this purpose the sampling strategy was based upon the comparison between contrasting stations located in the fertilized waters and in the surrounding off-plateau HNLC waters.

In this paper, we examine the silicon cycle in the surface waters of the two contrasting environments with particular emphasis on the impact of iron availability on the $Si(OH)_4$ uptake process and its consequences for the Si, C and N biogeochemical cycles. We address the following questions:

- What is the impact of Fe on the ability of natural diatom populations to use $Si(OH)_4$?
- What is the impact of Fe on Si:NO_3 and Si:C uptake ratios ?
- What are the consequences for the fate of the biogenic matter ?

2. Methods

2.1. Sampling strategy

The KEOPS cruise was conducted in the Kerguelen Isles region from 19 January to 13 February 2005, aboard the

R.V. *Marion Dufresne* (TAAF/IPEV). In order to compare the Si biogeochemical cycle within the surface layer between two contrasting environments, biogeochemical parameters were investigated at 18 stations encompassing three distinct transects: A, B and C (Fig. 1). Each transect covered a wide range of depths from stations above the plateau (bathymetry <1000 m) to off-plateau stations (bathymetry >1000 m). Two reference stations, A3 and C11, were, respectively defined for the plateau and the HNLC off-plateau area and were visited on several occasions. Rate measurements were conducted at three stations including the two reference stations A3 (three vertical profiles) and C11 (two profiles) and another station above the plateau (station B5, one profile). Irradiance data obtained at these three stations (range 28.3–32.4 mol quanta $m^{-2} d^{-1}$) show that the variability in light availability was low during the study (Uitz et al., in prep.). Table 1 synthesizes the station sampling dates and the exact geographical locations.

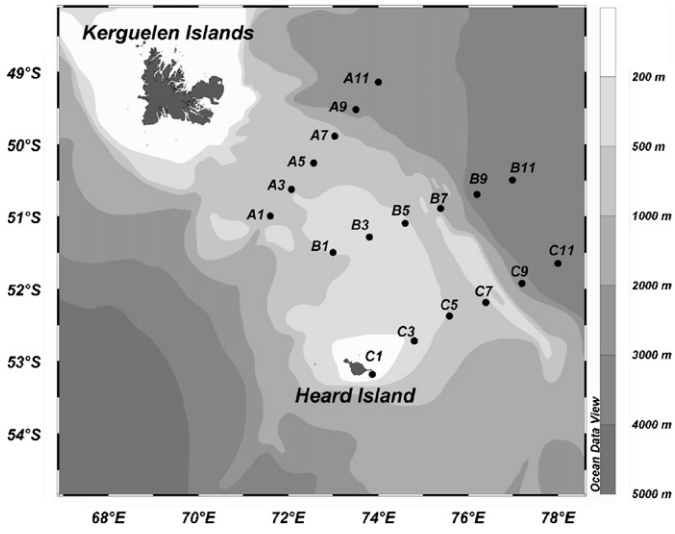

Fig. 1. Bathymetry of the study area and sampling stations.

Seawater samples were collected using a set of 24 Niskin bottles mounted on a rosette frame equipped with a Sea-Bird *SBE-911 plus* CTD sensor. Two kinds of CTD casts were conducted: some casts were dedicated to stock sampling only (referred to as stock-CTD) while the remainder were dedicated to sampling for both stock and rate measurements (referred to as flux-CTD) (Table 1). We sampled the entire water column for particulate silica during stock-CTD casts. During flux-CTD casts, sampling

Table 1
Station and transect sampling dates and location

	Station	Latitude/longitude	Date	CTD cast
Additional visit	A3-1	50.65°S, 72.08°E	01/19	Stock-CTD, flux-CTD
A transect	A11	49.14°S, 74.00°E	01/20	Stock-CTD
	A9	49.52°S, 73.50°E	01/23	Stock-CTD
	A7	49.89°S, 73.04°E	01/22	Stock-CTD
	A5	50.26°S, 42.57°E	01/22	Stock-CTD
	A3-2	50.62°S, 72.32°E	01/23	Stock-CTD
	A1	50.99°S, 71.60°E	01/23	Stock-CTD
Additional visit	A3-3	50.69°S, 71.99°E	01/24	Stock-CTD, flux-CTD
Additional visit	C11-1	51.64°S, 78.00°E	01/26	Stock-CTD, flux-CTD
Additional visit	C11-2	51.64°S, 78.00°E	01/28	Stock-CTD, flux-CTD
B transect	B11	50.49°S, 76.99°E	01/29	Stock-CTD
	B9	50.69°S, 76.20°E	01/30	Stock-CTD
	B7	50.89°S, 75.39°E	01/30	Stock-CTD
	B5	51.09°S, 74.60°E	02/02	Stock-CTD, flux-CTD
	B3	51.28°S, 73.80°E	02/02	Stock-CTD
	B1	51.50°S, 73.00°E	02/02	Stock-CTD
Additional visit	A3-4	50.65°S, 72.07°E	02/04	Stock-CTD, flux-CTD
C transect	C11-3	51.65°S, 78.00°E	02/06	Stock-CTD, flux-CTD (no Si flux measurement)
	C9	51.92°S, 77.20°E	02/06	Stock-CTD
	C7	52.19°S, 76.40°E	02/07	Stock-CTD
	C5	52.38°S, 75.59°E	02/07	Stock-CTD
	C3	52.72°S, 74.81°E	02/08	Stock-CTD
	C1	53.18°S, 73.87°E	02/09	Stock-CTD
Additional visit	A3-5	50.62°S, 72.09°E	02/12	Stock-CTD, flux-CTD (no Si flux measurement)

Distinction was made between stations sampled during the transects and during additional visits out of the transects. See text for details regarding measurements performed during CTD cast deployments.

was performed for $Si(OH)_4$ uptake rate profiles, for particulate silica profiles (depths corresponding to 100%, 50%, 25%, 8%, 4%, 1% and 0.1% of the surface Photosynthetically Active Radiation (PAR)) and for $Si(OH)_4$ uptake kinetic experiments (at surface and 1% PAR light level only). All samples were collected in polycarbonate NALGENE® bottles.

2.2. Sample treatments and measurements

2.2.1. Particulate silica stocks

For particulate silica, 1 l samples were filtered through 0.6-μm Nuclepore® polycarbonate filters. Size-fractionation (>10 μm and 0.6–10 μm) was achieved through cascading filtrations (0.6- and 10-μm Nuclepore® polycarbonate filters) for samples collected from the 100 and 1% PAR levels of the flux-CTD casts. Each filter was folded in quarters and placed in a petri dish. Biogenic and lithogenic silica concentrations were determined by a NaOH/HF digestion protocol modified from Brzezinski and Nelson (1995). Blank values were 6 ± 5 and 8 ± 4 nmol l^{-1} for the NaOH and HF digestion, respectively. The measurement precision, considered as three times the standard deviation of the blanks, is ~15 nmol l^{-1}. Lithogenic silica (LSi) interference on the measurement of BSi was quantified through the aluminium correction method (Ragueneau et al., 2005) for the set of samples obtained from flux-CTD casts. Aluminium was measured by ICP-AES. Results from these flux-CTD samples indicate that BSi correction from the LSi interference was generally low (7.3 ± 8.8%) for the study area, with exception to station C1 located in shallow waters near Heard Island (32.2 ± 8.4%). Due to the low LSi concentrations over the study area, LSi correction from labile LSi, which dissolved during the NaOH extraction, was high and variable. For these reasons, (1) we did not correct BSi concentration values of stock-CTD samples except for station C1, (2) we were unable to validate LSi concentrations for the stock-CTD samples as we could not apply an average correction factor on LSi values. Only LSi concentrations that were individually corrected from flux-CTD casts (0–200 m) are available. These LSi data are not presented in detail in this paper as the resolution of the profiles is very low. Nevertheless, we can constrain the LSi values at <0.7 μmol l^{-1} for all our samples, with exception again to station C1 (Heard Island) where higher values were clearly encountered.

2.2.2. Silica production rates

For silica production rate measurements 250 ml samples were collected before dawn, and spiked with 444 Bq (added volume = 20 μl) of a filtered (<0.2 μm) ^{32}Si radioisotopic solution (Los Alamos National Laboratory, specific activity = 23.5 kBq μg Si^{-1}). After tracer addition each sample was placed for 24 h in deckboard incubators cooled with circulating surface seawater and covered with nickel screens to simulate the photometric depths of collection. At the end of incubation periods samples were filtered onto 0.6-μm Nuclepore® polycarbonate filters, which were then rinsed with filtered seawater (<0.2 μm), and stored in plastic scintillation vials for radioactivity counting back in the laboratory. Size-fractionation filtration was performed as described above for particulate silica on samples collected and incubated at 100% and 1% PAR depths. Radioactivity was measured using a Packard 1600-TR scintillation counter once samples had reached secular equilibrium between ^{32}Si and its daughter isotope ^{32}P (~3 months delay). Counting was performed using the Cerenkov effect (Leynaert, 1993). All samples were counted in duplicate during a delay ensuring a counting precision $2\sigma<2.5$%. The counting duration was on average 68 mn (range 2–300 mn). Calculations of silica production rates (ρSi, in μmol l^{-1} d^{-1}) were then carried out according to Leynaert (1993):

$$\rho\mathrm{Si}\,\frac{A_f}{A_i}\times[\mathrm{Si(OH)_4}]\times\frac{24}{T}$$

with A_i and A_f (cpm) the initial and final activity of the samples, $[Si(OH)_4]$ the ambient concentration (the concentration of 0.003 μM ^{32}Si added is neglected) and T the duration (in hours) of incubation.

Si-specific uptake rates (V_{Si} in d^{-1}) were calculated as following:

$$V_{Si}=\rho\mathrm{Si}/\mathrm{BSi}.$$

2.2.3. Silicon uptake kinetics

For kinetic uptake experiments seven 100-ml samples, collected at each target depth, received increasing $Si(OH)_4$ additions. These samples were spiked with ^{32}Si, like samples for silica production rate measurements, and incubated over 8 h in deck incubators covered with appropriate light screens (100 or 1% PAR levels). After incubation, samples were filtered and stored as described for samples for silica production rate measurements. Kinetic parameters (K_S and V_{max}) were determined by fitting the data plot of Si-specific uptake rates as a function of silicic acid concentrations to a Michaelis-Menten's curve with a non-linear adjustment procedure (least-squares regression) using the Levenberg-Marquardt algorithm (Brooks, 1992).

2.3. Other parameters

In this paper, we will present abbreviated results of chlorophyll *a* (Chl *a*) and nutrient stocks as well as carbon and nitrogen production rates. Chl *a* and accessory pigment concentrations were measured by high performance liquid chromatography (HPLC) following the method described in Van Heukelem and Thomas (2001). Nitrate, silicic acid and phosphate concentrations were analysed with a Technicon autoanalyzer as described in Tréguer and Le Corre (1975). Ammonium concentrations were measured by a sensitive fluorimetric method (Holmes

et al., 1999). Measurements of carbon and nitrogen uptake rates as well as particulate organic carbon and nitrogen concentrations were obtained from flux-CTD water samples incubated simultaneously with ^{13}C and ^{15}N (Raimbault et al., 1999) in parallel with samples for silicon uptake rate measurements.

3. Results

3.1. Chl a and nutrient distributions in the two contrasted areas

Average profiles of Chl *a*, silicic acid, nitrate, and phosphate concentrations (Fig. 2A–D) from several visits at stations A3 and C11 clearly reveal that waters sampled at the two stations had different biogeochemical properties. Chl *a* biomass was higher above the plateau (1.1–2.1 $\mu g\,l^{-1}$ between 0 and 125 m at station A3) as compared to the off-plateau area (0.1–0.2 $\mu g\,l^{-1}$ between 0 and 125 m at station C11). Details of Chl *a* data for the entire set of stations are presented by Uitz et al. (in prep.).

At station C11, together with low Chl *a* concentrations, high levels of surface $Si(OH)_4$, NO_3^- and PO_4^{3-} concentrations, respectively averaging 25.1, 29.4 and 2.1 μM in the upper 80 m, were indicative of the HNLC conditions prevailing at this off-plateau area. At station A3 there was a large difference between the stock of silicic acid, which was quite depleted (average: 1.8 μM in the upper 80 m), and that of nitrate and phosphate, which were still high (average: 23.0 and 1.7 μM, respectively, in the upper 80 m). At the latitude of A3, winter nutrient concentrations, measured at the time-series station KERFIX (50.66°S, 68.42°E), were about 18 μM for $Si(OH)_4$ and 28 μM for NO_3^- (Pondaven et al., 2000). Comparison between winter and summer nutrient concentrations allows an assessment of the apparent seasonal nutrient consumption, which disregards the effects of advection and turbulent mixing. At station A3 a 3-fold larger decrease of $Si(OH)_4$ in comparison to NO_3^- characterized the nutrient pool evolution over the growth season. This means that in the bloom area a strong decoupling between $Si(OH)_4$ and NO_3^- utilization occurs.

Average ammonium (NH_4^+) profiles (Fig. 2E) indicated relatively large concentrations at station A3 marked by a peak of 1.9 μM at 125 m, coinciding with the Chl *a* maximum. NH_4^+ concentrations were lower at station C11, with peaks of 1.0 μM at 60 and 125 m. Large variations of NH_4^+ concentrations between the repeat visits were observed at the two reference stations.

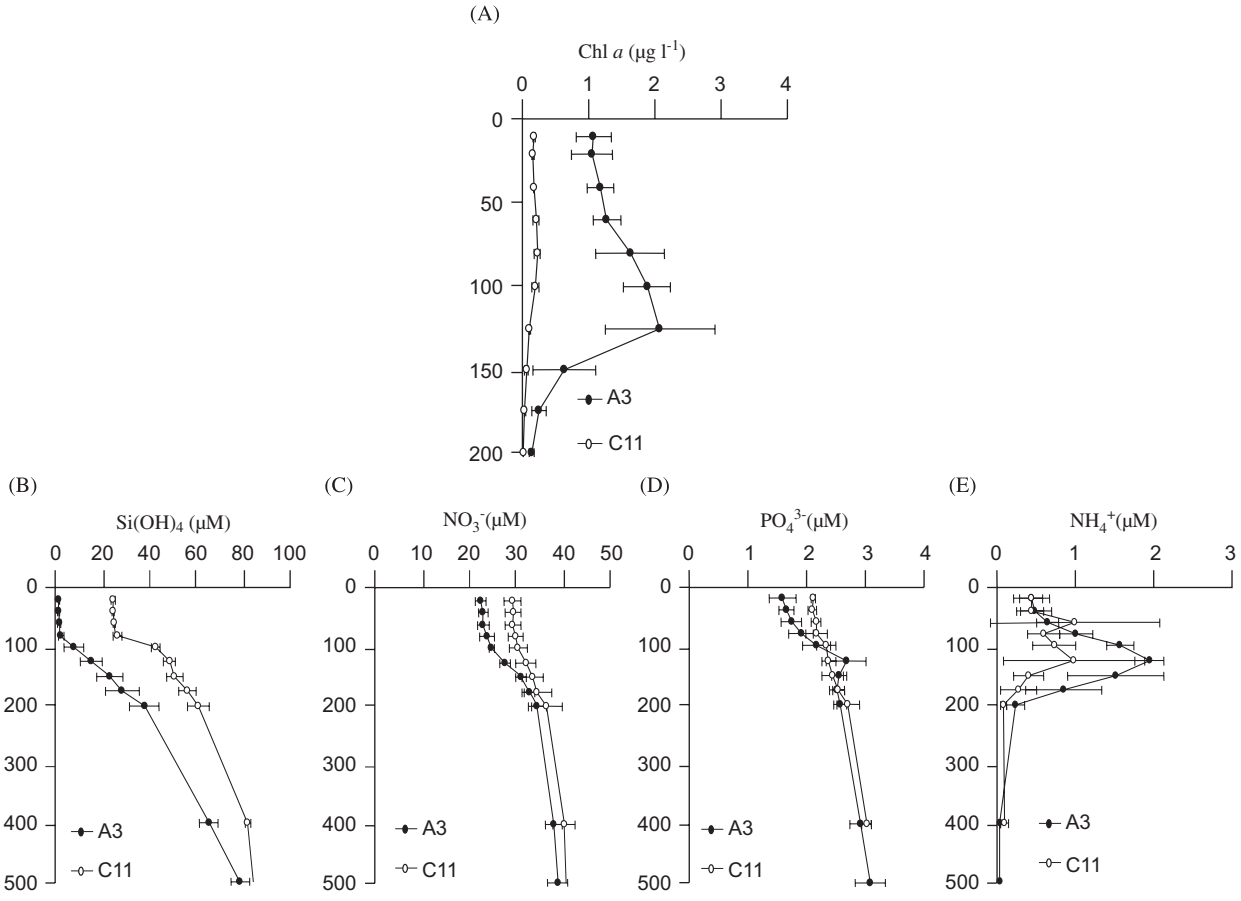

Fig. 2. Average profiles of (A) Chl *a*, (B) $Si(OH)_4$, (C) NO_3^-, (D) PO_4^{3-}, and (E) NH_4^+ concentrations from several visits at the two references stations A3 for the plateau area (filled symbols) and C11 for the off-plateau area (open symbols).

3.2. Biogenic silica concentrations

As shown in Fig. 3, BSi concentrations measured on transects A and B were clearly higher in the bloom area above the Kerguelen Plateau as compared to the off-plateau stations. BSi concentrations in the bloom were $>3\,\mu mol\,l^{-1}$ throughout the upper 100 m (transect B) or 200 m (transect A) whereas they were $<2\,\mu mol\,l^{-1}$ at off-plateau stations. The bloom area stations A1, A3 and A5 were characterized by especially high BSi concentrations (5–7 $\mu mol\,l^{-1}$) at ~100–150 m depth. On transect C, BSi concentrations were relatively low ($<2\,\mu mol\,l^{-1}$) except at station C1 (~3 $\mu mol\,l^{-1}$) and especially at the HNLC reference station (C11) where concentrations from 3 to 5 $\mu mol\,l^{-1}$ were detected between 0 and 100 m. Station C1 differed greatly from the other stations on this transect because of its proximity to Heard Island (Fig. 1) and its bathymetry (~200 m depth). Consequently, we will not discuss this station further in this paper.

BSi concentrations measured during the course of the transects were integrated between 0 and 200 m, independently of mixed-layer depth. This was done to take into

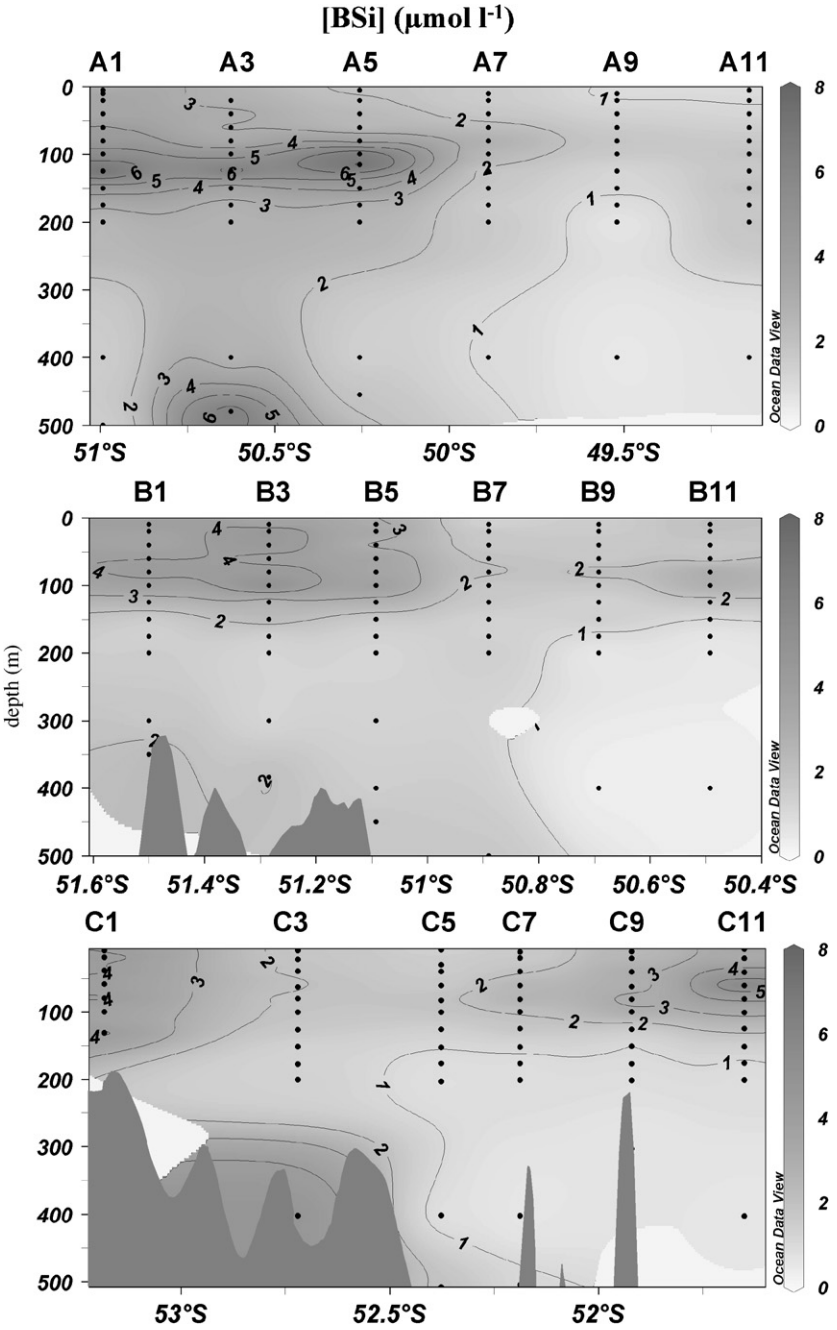

Fig. 3. Contours of biogenic silica concentrations between the surface and 500 m for each of the three transects. The dots indicate the spatial distribution of samples. In this figure, BSi concentration data at the two references stations A3 and C11 were taken from the visits made during the transects A and C (visits A3-2 and C11-3, see Table 1).

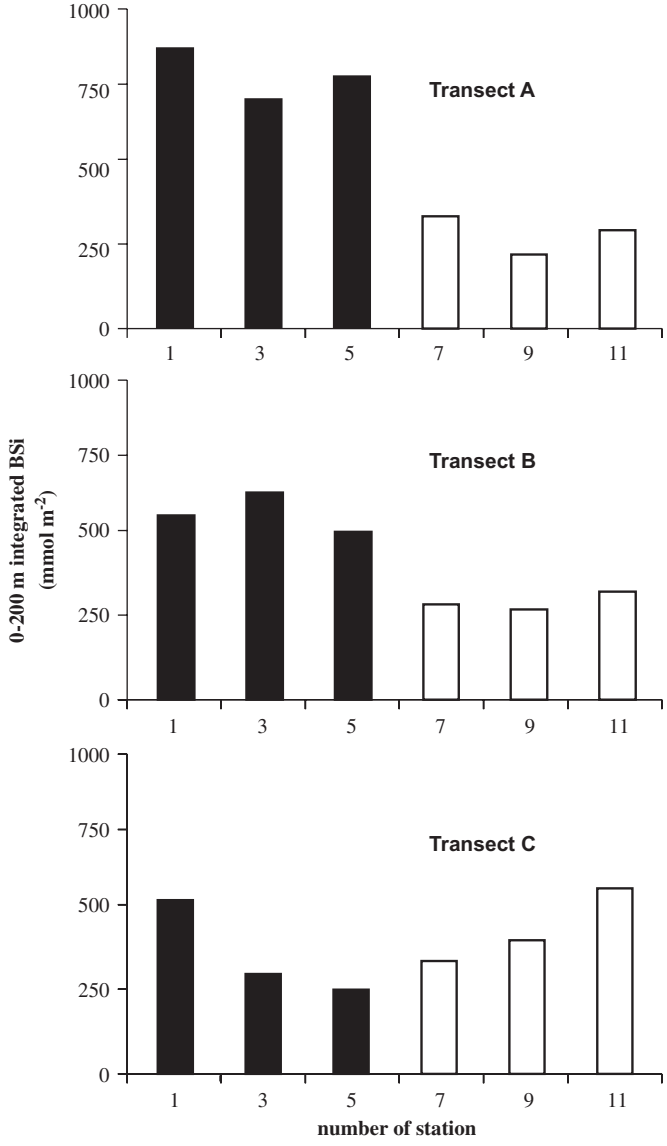

Fig. 4. Integrated BSi concentration (mmol m^{-2}) between 0 and 200 m for the stations above the plateau (black bars) and the stations off-plateau (white bars) visited during the course of transects A–C.

account the occurrence of biogenic material, as revealed from, e.g., Chl *a* (Uitz et al., in prep.) and BSi, between 100 and 200 m especially on the plateau area as noted above. Results show clearly the gradient of BSi concentration from the off-plateau HNLC to the plateau region (Fig. 4). However this trend is disrupted with a relatively high integrated BSi concentration at C11, as mentioned above for Fig. 3, reaching the same magnitude as above the plateau (e.g., stations B1, B5).

Fig. 5 presents the temporal evolution of BSi concentrations at the two contrasting reference stations A3 and C11. At station A3, which was sampled prior to the start of transect A, the main feature of temporal variability was the decline of the siliceous biomass concentrations from the first visit to the following ones. BSi concentrations were extremely high during the first visit to A3 with a maximum of 21.3 $\mu mol\,l^{-1}$ at 125 m which then declined in the course of the following visits, yet still exhibiting high values (ranging between 6.6 and 8.7 $\mu mol\,l^{-1}$). One can especially note the position of the siliceous biomass maximum, which was quite deep (125 m). BSi concentrations had already decreased at A3 when this station was sampled again during completion of the first transect. At station C11 BSi concentration temporal variability was low and the most striking feature was the relatively high BSi values in spite of its HNLC character (Fig. 5).

3.3. Silica production rates

Vertical profiles (Fig. 6) show that ρSi values were maximal at the surface and decreased with depth to non-zero values at the base of the euphotic zone like classical ρSi profiles. At station A3 surface ρSi decreased from 0.37 (A3-1) to 0.23 $\mu mol\,l^{-1}\,d^{-1}$ (A3-4). The highest value of surface ρSi was obtained at station B5 (0.52 $\mu mol\,l^{-1}\,d^{-1}$). At station C11 surface ρSi were 0.16 and 0.28 $\mu mol\,l^{-1}\,d^{-1}$ on the first and second visits, respectively. This indicates, apart from the first visit at station A3, that surface BSi

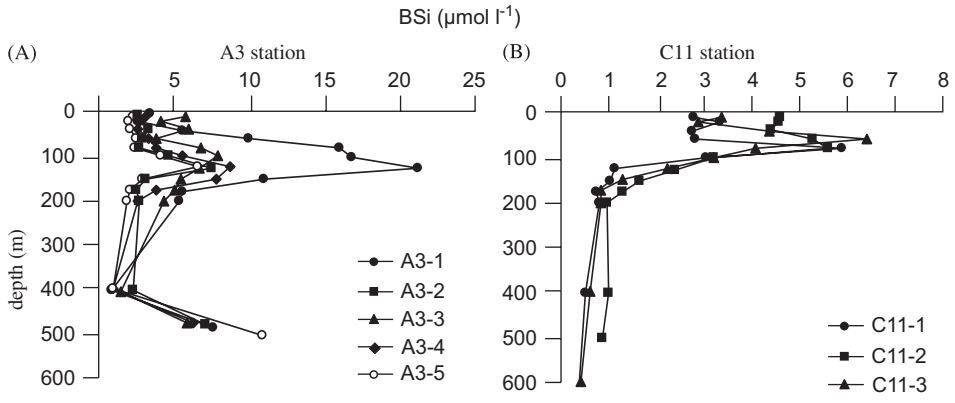

Fig. 5. Temporal variability of BSi concentrations from several visits at the two reference stations (A) A3 for the plateau area and (B) C11 for the off-plateau area.

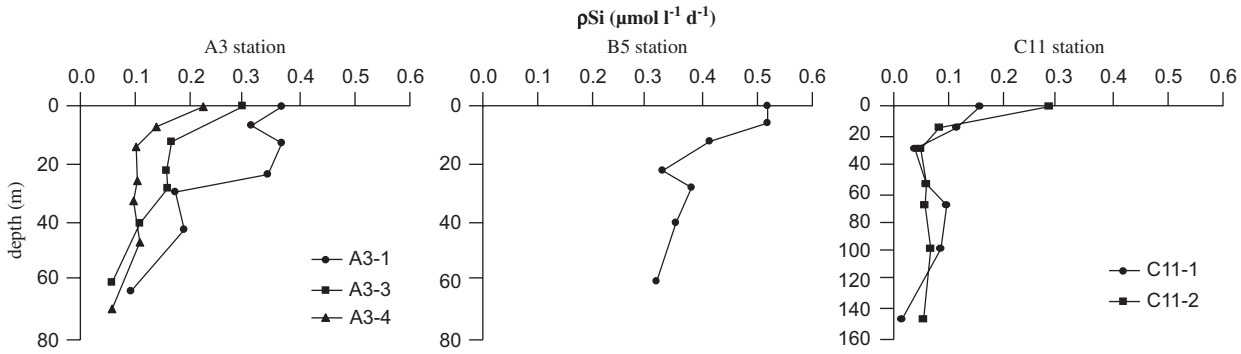

Fig. 6. BSi production rate profiles at the stations A3, B5 and C11.

Table 2
Integrated BSi production rate ($\Sigma\rho$Si) and averaged Si-specific uptake rate (ΣV_{Si}) values within the euphotic and the 0–40 m layers

Station	Euphotic layer depth (m)	$\Sigma\rho$Si euphotic layer (mmol $m^{-2} d^{-1}$)	$\Sigma\rho$Si 0–40 m (mmol $m^{-2} d^{-1}$)	ΣV_{Si} Euphotic layer (0–40 m) (d^{-1})
A3-1	42	11.9	11.9	0.08 (0.08)
A3-3	40	7.0	7.0	0.06 (0.06)
A3-4	46	5.5	4.8	0.04 (0.04)
A3 average		8.1 ± 3.4	7.9 ± 3.7	0.06 ± 0.02 (0.06 ± 0.02)
B5	40	16.1	16.1	0.10 (0.10)
C11-1	98	8.0	3.6	0.04 (0.04)
C11-2	98	7.5	4.2	0.03 (0.04)
C11 average		7.8	3.9	0.04 (0.04)

production rates were quite similar at the two contrasting reference stations. Si-specific uptake rates present the same trends (profiles not shown). Si-specific uptake rates (V_{Si}) at the surface varied temporally from 0.08 to 0.05 d^{-1} at station A3, reaching 0.11 d^{-1} at station B5, and varying temporally from 0.05 to 0.08 d^{-1} at station C11. Results of size-fractionated silica production indicate that large diatoms were clearly more active with regard to $Si(OH)_4$ uptake on the plateau area, whereas this trend was less clear in the HNLC area. No marked difference was observed between 100% and 1% PAR levels where size-fractionation had been examined. The >10 μm size-fraction at station A3 accounted for 99.0–96.2%, 99.1–91.1% and 78.3–68.0% of total Si uptake rate, respectively for the three successive visits and at the 100%–1% PAR levels. This size-fraction also accounted for 86.8–82.5% at station B5. At station C11 the larger size-fraction (>10 μm) accounted for 82.4–69.0% and 28.0–63.0% of Si production at the 100–1% PAR levels for the two first successive visits, respectively. Size-fractionation of BSi biomass carried out at the same depths as Si production size-fractionation revealed the major part of BSi biomass was present in the larger pool (>10 μm) independent of depth during the different visits to A3 (79.0–94.6%), B5 (90.5–90.9%) and C11 (71.2–82.4%).

Vertically integrated ρSi are reported in Table 2. Considering the large differences of the euphotic layer depth between the stations on the plateau (A3 and B5) and the HNLC station C11 we considered that comparison of vertically integrated Si uptake rates within the same water layer is more significant. Integrated ρSi rates from surface to 40 m ($^{40m}\Sigma\rho$Si) decreased over the course of the cruise from 11.9 to 4.8 mmol $m^{-2} d^{-1}$ at station A3 (average: $^{40m}\Sigma\rho Si = 7.9 \pm 3.7$ mmol $m^{-2} d^{-1}$). Following the trend already mentioned for vertical profiles $^{40m}\Sigma\rho$Si was higher at station B5 (16.1 mmol $m^{-2} d^{-1}$). At station C11 $^{40m}\Sigma\rho$Si did not show a major evolution over time with values ranging between 3.6 and 4.2 mmol $m^{-2} d^{-1}$, respectively, for the two consecutive visits. Averaged Si-specific uptake rates (ΣV_{Si}) showed similar trends: a temporal decrease of ΣV_{Si} at station A3 (from ~0.08 to 0.04 d^{-1}) towards a final value identical to values measured at C11 (~0.04 d^{-1}); and interestingly the highest ΣV_{Si} at station B5 (~0.10 d^{-1}). Correction of V_{Si} values from the contribution of only living cells to BSi [corrected $V_{Si} = \rho Si/(BSi \times \%living\ cells)$; %living cells are from Armand et al., 2008] is of minor importance with respective averaged values of 0.09, 0.07 and 0.05 d^{-1} at A3, 0.12 d^{-1} at B5, 0.05 (or 0.06) and 0.05 d^{-1} at C11 (see Table 2 for comparison).

3.4. Silicon uptake kinetics

Representative results of the size-fractionated silicon uptake kinetic experiments are presented in Fig. 7. Two kinds of silicon uptake trends were observed: in some cases

we had a clear hyperbolic evolution of Si-specific uptake rates with increasing silicic acid concentrations, whereas in other cases the evolution of Si-specific uptake rates was almost linear. The hyperbolic Si uptake kinetics were mostly observed at stations A3 and B5 and the linear ones were largely associated with station C11. Such a linear response of Si-specific uptake rates to silicic acid concentrations has been previously obtained (Brzezinski and Nelson, 1996; Brzezinski et al., 1998; Brown et al., 2003; Leblanc et al., 2005). In such conditions it is not possible to directly determine the kinetic parameters K_S and V_{max}. However, we can use a linear regression to fit a straight line through zero to the data set and consider the slope of the regression as an indicator of the diatom response to the increase of silicic acid. Indeed, as the slope of the linear regression is V_{Si} divided by the concentration of silicic acid and K_S is the concentration of silicic acid at $V_{Si} = V_{max}/2$ twice the value of the slope is equivalent to the affinity for silicic acid defined by $\alpha_{Si} = V_{max}/K_S$ (Healey, 1980). Consequently, in order to compare these different Si uptake kinetics between the contrasting stations in a homogenous way, all the affinities for silicic acid (α_{Si}) were determined by the use of such linear regressions. We made linear regressions of the entire data set for the linear kinetics and similarly linear regression of the initial slopes for the hyperbolic kinetics (Table 3). Affinities for silicic acid availability were clearly higher, regardless of the diatom size-fractionation, on the plateau as compared to the HNLC region. Focusing on the size-fractions, the smaller diatom size class presented higher (4-fold) affinities for silicic acid as compared to the larger size class.

Examination of the available individual kinetic parameters, K_S and V_{max}, at the bloom stations allowed us to delimit a range for these values. K_S values varied from 5 to 15 μM and V_{max} varied from 0.1 to 0.3 d^{-1} for the total diatom community. Regarding the size-fractions, kinetic parameters were in the range $K_S = 4$–11 μM, $V_{max} = 0.1$–0.3 d^{-1} for the large (>10 μm) fraction and

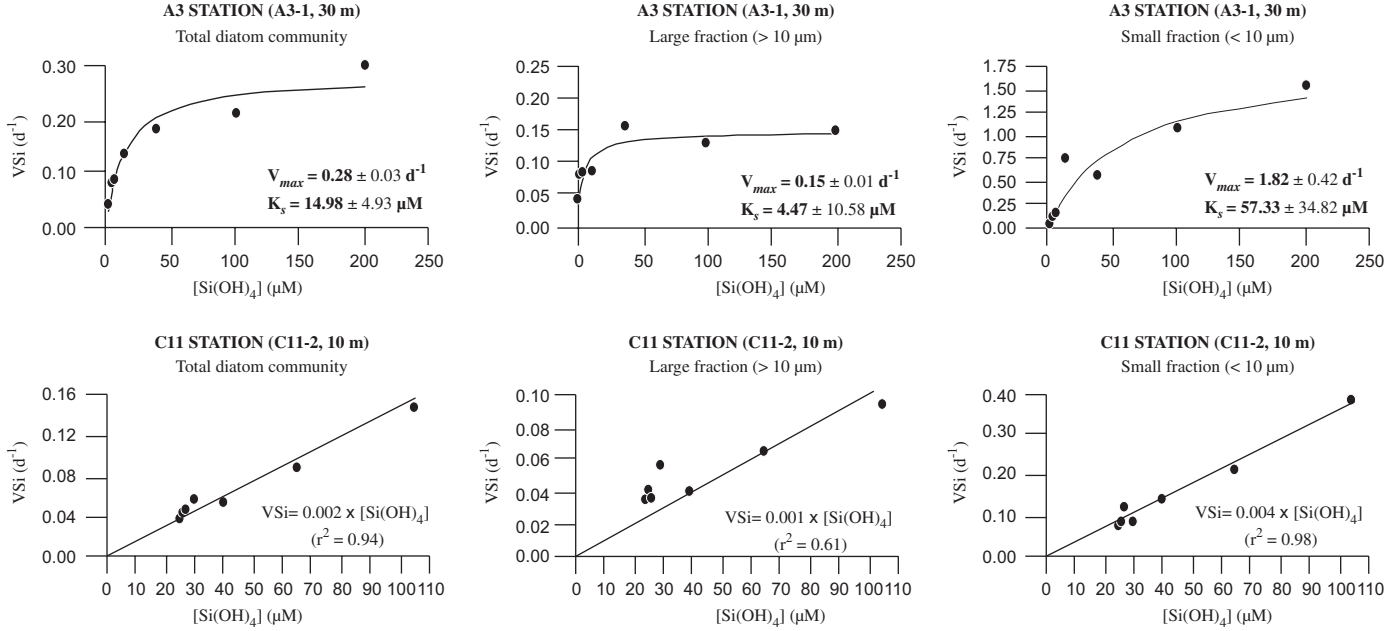

Fig. 7. Representative Si uptake kinetic curves obtained at the station A3 and C11 for the total diatom community and the two size fractions (>10 μm and <10 μm).

Table 3
Range of affinity for silicic acid (α_{Si}, $d^{-1}\,\mu M^{-1}$)

α_{Si} range ($d^{-1}\,\mu M^{-1}$)	Total diatom community	Size-fractions	
		Large fraction (>10 μm)	Small fraction (<10 μm)
Stations in the bloom area (A3 and B5)	0.026–0.070	0.034–0.038	0.160[a]–0.180
Station in the HNLC area (C11)	0.002–0.004	0.002–0.004	0.004–0.008

Only statistically significant values ($p > 0.95$) were taken into account.
[a]Non-significant values were comprised within the calculated range except for the lowest value of the small fraction range at A3 and B5 (0.024 and 0.042 $d^{-1}\,\mu M^{-1}$ as calculated from fitting to a Michaelis-Menten equation).

in the range $K_S = 27$–$57\,\mu M$, $V_{max} = 0.4$–$3.9\,d^{-1}$ for the small (<10 μm) fraction. This indicates that, in addition to higher affinities for $Si(OH)_4$, the small fraction experienced higher K_S and V_{max} values as compared to the larger size-fraction.

In each hyperbolic Si uptake kinetic obtained for the plateau stations, regardless of the size-fraction, K_S values were always higher than the ambient silicic acid concentration. This indicates that diatom silicification was limited by external silicic acid concentrations in the bloom, and probably growth rate as well—based on comparison to other studies reporting that the half-saturation constant for growth is generally 10–20% of the K_S value (e.g., Nelson and Dortch, 1996; Nelson et al., 2001). In relation to the linear Si uptake kinetics at the HNLC station C11, in each case the V_{Si} at ambient silicic acid concentration was inferior (16–84%) to the specific uptake rate obtained at the maximum addition of the nutrient, being clearly indicative of limitation by external $Si(OH)_4$ concentrations.

Table 4
Carbon and nitrogen (NO_3^-, NH_4^+) integrated uptake rates within the euphotic layer and relative contribution to the large size-fraction (>10 μm) at stations A3, B5 and C11

	A3 station	B5 station	C11 station
$\Sigma\rho C$ (mmol $m^{-2}\,d^{-1}$)	82.3±4.8	81.8	22.3±4.5
Range	75.8–86.1	n.d	17.3–25.9
$\Sigma\rho C$ >10 μm (%)	79.2±9.5	82.7	34.2±7.0
Range (%)	65.7–86.1	n.d	27.9–41.7
$\Sigma\rho NO_3$ (mmol $m^{-2}\,d^{-1}$)	4.5±2.7	5.5	1.7±0.4
Range	1.9–7.2	n.d	1.3–2.0
$\Sigma\rho NO_3$ >10 μm (%)	71.8±14.8	82.1	11.5±4.9
Range (%)	50.7–85.1	n.d	7.3–17.0
$\Sigma\rho NH_4$ (mmol $m^{-2}\,d^{-1}$)	5.5±1.2	3.7	3.9±0.2
Range	4.1–6.5	n.d	3.7–4.2
$\Sigma\rho NH_4$ >10 μm (%)	68.6±8.1	65.1	36.9±7.3
Range (%)	61.4–77.7	n.d	29.2–43.7

Values were averaged over four visits at station A3 (A3-1, A3-3, A3-4, A3-5) and three visits at station C11. Only one profile for each parameter was performed at station B5.

3.5. Silicon relative to carbon and nitrogen uptake ratios

A comparison of our silica production rates with those for carbon and nitrogen (Table 4) allowed us to investigate molar uptake ratios of these elements. Fig. 8 presents the profiles and integrated values of $\rho Si{:}\rho C$ and $\rho Si{:}\rho NO_3$ uptake molar ratios at stations A3, B5 and C11. The integrated $\rho Si{:}\rho C$ ratio decreased from 0.14 to 0.06 at station A3 and reached the value of 0.20 at station B5. The highest values of $\rho Si{:}\rho C$ were observed at station C11 (0.34–0.44). Integrated $\rho Si{:}\rho NO_3$ ratios were on average 1.6±0.5 (range 1.09–2.10) at station A3 and 2.95 at station B5. Again station C11 presented the highest $\rho Si{:}\rho NO_3$ with values ranging between 3.96 and 5.92.

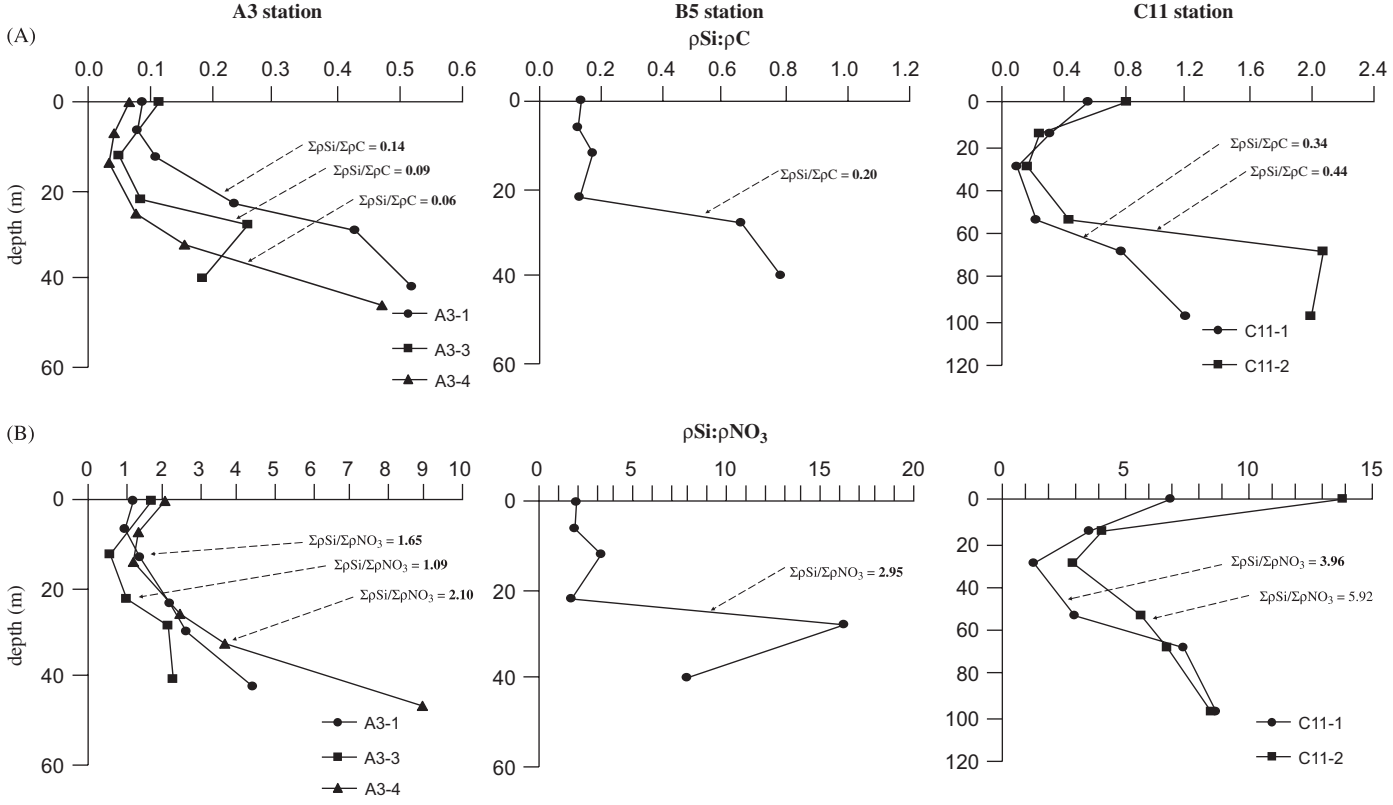

Fig. 8. Profiles of (A) Si:C and (B) $Si{:}NO_3$ uptake molar ratios at the stations A3, B5 and C11. Integrated ratio values are noted on the corresponding figures. Note the change of scale between figures.

4. Discussion

The investigations carried out during KEOPS above the Kerguelen Plateau provide insights into how natural and continuous iron-fertilization influences bloom properties and dynamics, i.e. its characteristics, evolution and fate. In the following section, the main features and the control factors of the silicon cycle and of the diatom bloom are discussed focusing on comparison between the bloom area and the off-plateau HNLC area on one hand, and comparison between natural and artificial iron fertilization, on the other hand.

4.1. Features of the silicon biogeochemical cycle in the naturally iron-enriched bloom region

A massive bloom was observed on the Kerguelen Plateau in the course of the 2005 austral summer. This bloom was almost exclusively composed of relatively large diatoms (Armand et al., 2008) in spite of low concentrations of silicic acid ($<2\,\mu M$ at the reference station A3). At station A3, particularly high BSi biomass (maximum concentration up to $20.0\,\mu mol\,l^{-1}$) was measured at the beginning of the cruise. Such a high level of BSi is in the same order of magnitude as maximum BSi values ranging from 16.0 to $11.7\,\mu mol\,l^{-1}$ for blooms occuring near the Polar Front (Quéguiner et al., 1997; Brzezinski et al., 2001; Quéguiner and Brzezinski, 2002). High BSi persisted in the surface layer throughout the studied period. The maximum concentrations at A3 decreased from 21.3 to $6.6\,\mu mol\,l^{-1}$ from the beginning to the end of the cruise. For the entire period investigated, integrated BSi concentration at A3 was on average $1100\pm600\,mmol\,m^{-2}$. At the beginning of the cruise BSi biomass was $2105\,mmol\,m^{-2}$ and at the last visit (A3-5) it was still as high as $605\,mmol\,m^{-2}$. As a comparison, during the two latter studies mentioned above, integrated BSi concentrations at the time of maximum biomass were on average $390\pm$ mmol m^{-2} in January 1998 (Brzezinski et al., 2001) and $870\pm270\,mmol\,m^{-2}$ in November 1992 (Quéguiner and Brzezinski, 2002). An additional study, during a massive bloom induced by receding ice-edge in the Ross Sea revealed an integrated BSi concentration of $1180\pm240\,mmol\,m^{-2}$ (Smith and Nelson, 1986). These results indicate that the BSi biomass we observed in our study was unusually high, even for the Southern Ocean.

BSi biomass was high below the mixed layer. Maximum concentrations ($6.6–21.3\,\mu mol\,l^{-1}$) were observed as deep as 125 m, where Chl *a* (Fig. 2A) and fucoxanthin (Uitz et al., in prep.) were also at a maximum. The chlorophyll degradation compounds such as chlorophyllides are mainly indicative of scenescent cells and phaeopigments (phaeophorbides + phaeophytines) resulting from grazing activity (e.g., Jeffrey et al., 1997). At 125 m, the ratio of Chl *a*/(Chl *a* + chlorophyllides) of particulate matter indicate that fresh material contributed on average 90% of the biomass. Total chlorophyll *a* is the sum of Chl *a* and chlorophyllides; the ratio of TChl *a*/(TChl *a* + phaeopigments) of particulate matter indicates that on average 94% of the biomass was living at 125 m.

Finally, diatom microscopic enumeration revealed diatom thanatocoenoses (i.e. dead cells, which we identified as empty frustules devoid of internal contents) of 15%, 16%, and 23% at 100 m to stations A3-3, A3-4, and A3-5, respectively (Armand et al., 2008). The occurrence of high living-diatom biomass below the euphotic layer could result from the accumulation of sedimenting diatoms; or alternatively as populations living at depth, since the maximum biomass was located within the nutricline. Higher $Si(OH)_4$ availability at depth could favour the growth of diatoms at depth, especially considering the near $Si(OH)_4$-depletion in the surface water (Fig. 2B). Light availability is extremely low at this depth ($<0.1\%$ of the surface incident light) and this can seriously hamper diatom growth although some studies have observed diatom growth below the euphotic zone (Nelson and Goering, 1978; Brzezinski and Nelson, 1989). We cannot resolve if the diatoms at the deep biomass maximum were actively growing or freshly sedimenting, as we did not investigate Si nor C production rates at these depths.

In spite of the high BSi biomass at our first arrival on the plateau, the diatom bloom was already in an advanced stage and then declined over the duration of the cruise (as shown by Chl *a* satellite images; Blain et al., 2007). Indeed, at A3, ρSi and V_{Si} were relatively low at the beginning of our study and decreased further until the end of the sampling period. The ρSi values we measured in the Kerguelen bloom area (average: $7.9\pm3.7\,mmol\,m^{-2}\,d^{-1}$, range: $4.8–11.9\,mmol\,m^{-2}\,d^{-1}$) are quite low as compared to those reported previously in Southern Ocean diatom blooms at this latitude. In the Polar Front region Quéguiner and Brzezinski (2002) found on average $30.6\pm16.1\,mmol\,Si\,m^{-2}\,d^{-1}$ in spring (range $29.6–60.7\,mmol\,m^{-2}\,d^{-1}$) and Brzezinski et al. (2001) found on average $22.6\pm20.0\,mmol\,m^{-2}\,d^{-1}$ in summer (range: $7.0–45.5\,mmol\,m^{-2}\,d^{-1}$). During this latter study surface silica production rate of up to $1.5\,\mu mol\,l^{-1}\,d^{-1}$ were measured within the bloom, whereas our maximum measured surface silica production rate value at station A3 was only $0.4\,\mu mol\,l^{-1}\,d^{-1}$. It is important to note that these relatively low Si production values may reflect the end phase of the productive period (i.e. the last active stage of the diatom bloom in the seasonal cycle) in this area. Satellite Chl *a* data (Blain et al., 2007) indicate that the bloom had started months earlier, in November 2004. We assume then that the high level of BSi biomass we observed at our first visit is representative of BSi production considerably higher prior to our investigation. The most striking feature of silicon cycling is that the diatom bloom is still able to persist in waters that are quite depleted in $Si(OH)_4$. The vertical diffusive flux of silicic acid above the plateau might help to sustain this bloom. The decrease of Si productivity during the study period was associated with a change in diatom community structure shifting from an

initial bloom of *Chaetoceros Hyalochaete* spp. to a quite monospecific bloom of *Eucampia antarctica* (Armand et al., 2008). The change is likely to have occurred around end of January–early February, as the diatom community structure change reported here was detected between the two successive visits of A3-3 and A3-4.

In parallel to the decay of the bloom at A3 there was a spatial shift of the Chl *a* maximum to station B5 where a bloom was observed beginning on 25 January. This bloom was mainly dominated in abundance by the same species *Chaetoceros Hyalochaete* spp. (Armand et al., 2008) observed at the beginning of our investigation at station A3. The integrated BSi biomass between 0 and 200 m at B5 was 536 mmol m^{-2} while $^{40m}\Sigma\rho Si$ was 16.1 mmol m^{-2} d^{-1}, a value much higher than A3 values. Silicic acid surface concentrations were relatively low, around 3.5–4.5 μM in the upper 80 m. However, this value is approximately 2 times greater compared to $Si(OH)_4$ surface concentrations at A3. This diatom bloom at the end of January may have been triggered by enhanced vertical mixing supplying sufficient silicic acid and iron to reinitiate diatom productivity. In addition to internal wave activity, vertical mixing might result from a deepening of the mixed layer due to high wind events characterizing the study area.

In contrast, there was little seasonal bloom development within the HNLC off-plateau region (0.2 μg l^{-1} maximum Chl *a* at C11). However, at C11 BSi biomass was relatively high: BSi maximum was 6.4 μmol l^{-1} and the 0–200 m integrated BSi concentration (570 ± 100 mmol m^{-2}) was equivalent to BSi biomass measured at station B5 (540 mmol m^{-2}). When integrated over the same depth, the silica daily production as well as the specific uptake rates were only ~50% lower as compared to the plateau (A3). It is not really clear what size-fraction of diatoms was contributing most to the Si production rates at this station due to the large variability of size class relative contribution we observed. Uptake of carbon and nitrogen was mainly driven by the small size-fraction (Table 4), and although it could not be totally due to diatoms, we think that Si production by small diatoms could also be quite important if not dominant under HNLC conditions. In that regard, Armand et al. (2008) found that the small diatoms *Fragilariopsis pseudonana* and *Cylindrotheca closterium* dominated in abundance although larger ones (*Fragilariopsis kerguelensis, Thalassiosira lentiginosa* and *Thalassiothrix antarctica*) dominated the biomass.

4.2. Impact of iron on silicon uptake efficiency

Most of the research investigating kinetic parameters of silicon uptake to date have used diatom community bulk measurements that do not distinguish between individual groups, i.e. size classes or species. However, using a Michaelis-Menten curve adjustment on a data set for the total phytoplanktonic community could introduce some biases and, especially, hinder large differences between algae as the uptake parameters probably differ between species. We investigated size-fractionated Si uptake kinetics to monitor differences between large (>10 μm) and small (<10 μm) diatoms.

Our kinetic experiments demonstrated that $Si(OH)_4$ ambient concentrations were limiting silica production across the entire study area including both the fertilized and HNLC waters, since adding silicic acid clearly increased silica-specific production rates. At stations A3 and B5, V_{Si} at ambient concentrations for the total diatom community were between 5% and 20% of V_{max}. Such a calculation cannot be made for station C11 as saturation of V_{Si} was never reached. Si-limiting conditions in the bloom area during the summer period reflect the observed level of $Si(OH)_4$ concentrations. Although the exact physiological reason remains unclear, a mesocosm study by Egge and Aksnes (1992) demonstrated that diatom dominance of a phytoplankton community vanished rapidly as silicic acid concentrations dropped below 2 μmol l^{-1}. This raises the question of how the diatom bloom community could persist over the Kerguelen Plateau area, even though silicic acid ambient concentrations were low and limiting. One key point is that some deep $Si(OH)_4$ stocks supplied from mixing process could sustain a part of Si production. From our kinetic experiments we demonstrated that α_{Si} values for silicic acid were clearly higher in the bloom area as compared to the HNLC area. Such higher affinities for $Si(OH)_4$ would indicate that diatoms in the bloom area were capable of surviving under low $Si(OH)_4$ conditions as compared to diatoms growing in the HNLC area. This is in agreement with the results of the artificial *in situ* fertilization experiment SOFeX (Brzezinski et al., 2005). The increase in affinity for silicic acid under Fe-enriched as compared to Fe-limited conditions could result from both changes in K_S and V_{max}.

During KEOPS, K_S values were lower in the Fe-enriched area similar to that observed in the SOFeX experiment. In the KEOPS HNLC area the observed linear response of V_{Si} to $Si(OH)_4$ concentrations could be representative of the first part of an hyperbolic curve. This in turn implies that K_S values would be very high and as such >55 μM, as no indication of saturation could be detected at the maximum tested $Si(OH)_4$ concentration of 110 μM. Such elevated K_S values have already been observed in Southern Ocean diatoms (Nelson and Tréguer, 1992; Nelson et al., 2001). This observation implies that K_S values of the naturally fertilized bloom (range 5–15 μM, for the total diatom community) were actually lower in comparison to the very high K_S values of the HNLC area. For the latter, the lack of saturation of V_{Si} suggests that V_{max} were higher than the maximal V_{Si} value (0.10–0.25 d^{-1} for the total diatom community) we obtained. In the bloom area V_{max} values ranged between 0.10 and 0.30 d^{-1} and did not differ substantially from the values in the HNLC area. From a general point of view V_{max} values are low across the study area, but this could reflect some very different situations: a strong limitation by silicic acid in the HNLC system and a declining diatom bloom in the iron-fertilized

area. Nevertheless, in combination with the $Si(OH)_4$ supply by vertical mixing, the high affinities for silicic acid over the plateau could explain the persistence of the diatom bloom in low $Si(OH)_4$ surface waters. As deduced from the size-fractionation, small diatoms presented the highest affinities for $Si(OH)_4$, although large diatoms clearly dominated the siliceous biomass. This could be interpreted as an indication of a preferential control by grazing on the small size-fraction as suggested from previous studies (Cullen, 1991; Morel et al., 1991).

Over the course of the KEOPS cruise we observed a shift in the dominance of the diatom community at station A3 from a mixed *Chaetoceros* spp., *Thalassionema nitzschioides. Fragilariopsis nitzschioides* and *F. kerguelensis* bloom to a quite monospecific population of *Eucampia antarctica*. The change in community structure could be related to the species-specific capacity in taking up silicic acid at continuously decreasing concentrations. Indeed, examination of the statistically significant estimates of α_{Si} (range shown in Table 3) suggests an increasing trend along the course of the sampling period from initially lower values ($\sim 0.3\,d^{-1}\,\mu M^{-1}$, A3-1) to finally higher values (~ 0.6–$0.7\,d^{-1}\,\mu M^{-1}$, A3-4) at the end of the study period. One factor favouring efficient nutrient uptake is high surface/volume (S/V) ratio (e.g., Sarthou et al., 2005), but measurements of the *E. antarctica* frustules (Cornet-Barthaux et al., 2007) revealed lower S/V ratios ($0.3 \pm 0.1\,\mu m^{-1}$, from 156 measurements) as compared to the *Chaetoceros* spp. ($0.7 \pm 0.3\,\mu m^{-1}$, from 172 measurements). Thus, the S/V ratio does not appear to have been a controlling factor in the bloom evolution, and other physiological adaptations or processes are probably of major importance including the areal density of silicic acid membrane-bound transporters (Aksnes and Egge, 1991), the differential affinities of the latter for $Si(OH)_4$ (Martin-Jézéquel et al., 2000) or a species-specific capacity for adjustment in the degree of silicification (Ragueneau et al., 2000).

Diatoms observed in HNLC areas are generally heavily silicified species (Smetacek et al., 2004). At C11, high integrated $\rho Si{:}\rho NO_3$ and $\rho Si{:}\rho C$ uptake ratios (Fig. 8) may reflect such a strong degree of silicification in iron-limited diatoms. We calculated the amount of BSi per diatom cell surface [BSi per cell surface = BSi concentration/(surface per cell × cell abundance)] using diatom measurements (Cornet-Barthaux et al., 2007) of species for which abundances in the diatom community were >1%. This calculation was made for mixed-layer diatom populations at 50 m depth. Results indicate that the degree of silicification was higher at station C11 (8–$21 \times 10^{-15}\,mol\,\mu m^{-2}$, visits C11-1 and C11-3) as compared to station A3 (4–$6 \times 10^{-15}\,mol\,\mu m^{-2}$, visits A3-1 and A3-5). Another indication of the silicification status of diatoms can be derived from BSi/fucoxanthin ratios, assuming that BSi is largely representative of living diatoms. This ratio was on average 5 times higher between 0 and 100 m depth at station C11 ($25.0 \pm 3.7\,mol\,g^{-1}$) in comparison to station A3 ($5.7 \pm 1.1\,mol\,g^{-1}$). However, microscopic examination (see Fig. 2; Armand et al., 2008) revealed that although the major part of the BSi biomass was associated with living biomass, detrital material cannot be completely neglected, with dead cells in the 0–100 m surface layer contributing on average to $15 \pm 4\%$ (8–23%) of diatom cells at A3 and $27 \pm 9\%$ (18–40%) of diatom cells at C11. Accounting of living cells only, the BSi/fucoxanthin ratios would be lower but still contrasted between the two stations ($4.9 \pm 1.0\,mol\,g^{-1}$ at A3 versus $18.2 \pm 2.7\,mol\,g^{-1}$ at C11). A stronger degree of silicification of diatoms living in HNLC waters is in agreement with their nutritional limitation by both silicic acid and iron availability resulting in a slower cell cycle, whose length plays the major role in controlling the silicification process (Claquin et al., 2002).

4.3. Impact of iron on $Si{:}NO_3$ uptake ratios

Since the first reports by Hutchins and Bruland (1998) and Takeda (1998) from bottle-enrichment experiments, high $Si{:}NO_3$ and Si:C uptake ratios have been widely reported for Fe-stressed algae from HNLC areas (Franck et al., 2000; Brzezinski et al., 2001; Quéguiner and Brzezinski, 2002; Franck et al., 2005). Artificial Fe-addition microcosm experiments (Hutchins and Bruland, 1998; Takeda, 1998; De La Rocha et al., 2000; Franck et al., 2000, 2005) indicated that alleviation of Fe limitation could reduce these ratios and generally drive them to near average values for healthy diatoms ($Si{:}NO_3$ ~1, Si:C ~0.13; Brzezinski, 1985). The KEOPS experiment offers the unique opportunity to address the question of $Si{:}NO_3$ and Si:C uptake ratios in relation to Fe availability in contrasting natural diatom communities. In this section we focus on the $Si{:}NO_3$ uptake ratios; Si:C uptake ratios will be discussed in the subsequent section addressing the functioning of the carbon biological pump.

At station A3, the average depth-integrated $\rho Si{:}\rho NO_3$ uptake ratio (1.6 ± 0.5, $n = 3$) was closer to the typical ratio of 1 assumed for healthy diatoms, in distinct contrast to the HNLC area (average 4.9 ± 1.0, $n = 2$). This trend is more poignant when considering the integration of uptake rates above the 25% surface irradiance level taking into account NO_3^- uptake could be limited by light availability at depth (1.2 ± 0.3 at A3 versus 5.0 ± 1.4 at C11). We do not have the values of regeneration (i.e. dissolution) rates for Si but, given the low temperatures throughout the region, dissolution is unlikely to have greatly biased the observed spatial differences.

The close to 1 ratios of $\rho Si{:}\rho NO_3$ measured through 24 h incubations at A3 are consistent with the occurrence of non-iron-limited diatoms above the plateau but does not help to explain the seasonal apparent decoupling of $Si(OH)_4$ and NO_3^- utilization and the large amount of remaining NO_3^- at the end of the productive season. The vertical supply of these two nutrients by the action of internal tides would even increase the decoupling, as the deep waters of the region are classically enriched in

$Si(OH)_4$ relative to NO_3^-. Given the vertical gradients of these latters (Fig. 2B, C), the silicic acid supply rate to the surface at station A3 (vertical concentration gradient between 100 and 200 m × vertical diffusivity coefficient K_Z; Park et al., 2008) is estimated to be 3 times higher than the nitrate supply rate (8.5 ± 1.4 mmol m^{-2} d^{-1} for $Si(OH)_4$ and 2.8 ± 0.5 mmol m^{-2} d^{-1} for NO_3^-, for the different visits).

The contrasted conclusions about $Si(OH)_4$ and NO_3^- relative utilization deduced from short-term flux measurements versus seasonal budget can result from the different temporal scales and methodologies involved. The uptake ratios that we measured in bottles are representative of the bloom status at its end while the nutrient stock ratios that we deduced from *in situ* observations are representative of the bloom story over months. For the latter, the high $Si(OH)_4$:NO_3^- utilization ratio could result from three different factors: (1) nitrate utilization, but not silicic acid uptake, could be limited by light availability at depth, as discussed above; (2) the high seasonal silicic acid relative to nitrate utilization could indicate that the bloom above the Kerguelen plateau was Fe-limited during earlier in the year, and (3) more rapid recycling of nitrogen than silicon may decouple uptake ratios from export ratios from the mixed layer. Iron limitation appears unlikely, but there is evidence of rapid nitrogen cycling.

Previous work has found iron limitation under conditions of relatively high iron supply. Hutchins et al. (1998) found varying degrees of Fe limitation in the California coastal upwelling area going along a continuum from fully Fe-replete to severely Fe-limited conditions. Boyd et al. (2005) observed during the artificial iron-addition experiment SERIES the progressive transition from an iron-replete to an iron-limited bloom and the resulting increase in the $Si(OH)_4$:NO_3^- drawdown ratio. However, in the KEOPS bloom, it appears that iron supply was not limiting. Blain et al. (2007, 2008) constrained the total iron supply from both the vertical diffusive flux and the winter stock above the plateau in the range 83–275 nmol m^{-2} d^{-1}. These estimates, which do not take into account the possible additional supply by dissolution of particulate Fe, show that the iron supply above the plateau was probably sufficient to account for the phytoplankton net iron demand of 208 ± 77 nmol m^{-2} d^{-1} estimated by Sarthou et al. (2008). Although the bioavailability of iron is complex and difficult to assess, the presence of organic ligands in excess of dissolved Fe concentrations (Gerringa et al., 2008) suggests that a large high amount of iron was bioavailable to phytoplankton. That is in accordance with the high F_v/F_m ratio (>0.5) measured from visits A3-1 to A3-4 (Timmermans, pers. comm.) indicating a relatively good physiological status of the phytoplankton community. We cannot really exclude that a small degree of iron limitation might have existed over the Kerguelen Plateau, but it is unlikely to explain the large (factor 3) decoupling of $Si(OH)_4$:NO_3^- utilization over the bloom development that appears typical of Fe-depleted areas (Hutchins et al., 1998; Boyd et al., 2005).

More rapid recycling of nitrogen than silicon appears to have been important. A high contribution of NH_4^+ to total N uptake rates in the bloom could balance the relatively low NO_3^- uptake: at station A3, with rates of 4.1–6.5 mmol m^{-2} d^{-1} (Table 4) NH_4^+ uptake accounted for 39–77% (57%, on average) of the total N uptake. At station A3, NH_4^+ was rapidly made available due to the high activity of the heterotrophic community. The mesozooplankton biomass was very large in the core of the bloom (8.9–10.8 g C m^{-2}, at station A3) and the community was well established with the occurrence of all stages of copepod development (Carlotti et al., 2008). Bacterial abundance and production were also very high, and ~70% of the primary production passed through heterotrophic bacteria (Obernosterer et al., 2008).

By comparison, in HNLC waters NH_4^+ uptake accounting for 71 ± 6% of the total N uptake also overwhelmed NO_3^- uptake at station C11, although the heterotrophic community was less abundant. Mesozooplankton and bacteria biomass were, respectively, 3- and 2-fold less important as compared to those measured at station A3 (Carlotti et al., 2008; Obernosterer et al., 2008). The importance of NH_4^+ over NO_3^- uptake is a classical situation of HNLC Fe-limited systems (see, for instance, Brzezinski et al., 2003) but the situation was quite surprising for the Fe-fertilized area where the low seasonal consumption of NO_3^- was concomitant to a preferential uptake of NH_4^+ by diatoms. A physiological preference for NH_4^+ is presumably derived from an energetic advantage, as reduction of NO_3^- to the oxidation level of organic N requires the equivalent of 8 electrons, while NH_4^+ is already reduced. Thompson et al. (1989) showed these energetic considerations are more complex considering other factors in play such as light or substrate availability and adaptative strategies to sustain a high growth rate. Inhibition of NO_3^- uptake by large amounts of recycled NH_4^+ has also been invoked (e.g., Wheeler and Kokkinakis, 1990), although this behaviour is not yet fully resolved (Dortch, 1990).

The examination of ρSi:ρNO_3 uptake ratios (i.e. from both short-term fluxes and seasonal drawdown) can be interpreted in the light of the net production of matter that can be exported out of the euphotic layer because NO_3^--based production represents the net N production in the Southern Ocean (Brzezinski et al., 2003), while our ρSi estimates are close to net production of biogenic silica due to low dissolution rates. The link between nutrient utilization and export of organic matter is not direct, as the high diatom biomass that has accumulated in the surface could strongly affect the export ratio. A calculation accounting of the nutrient seasonal depletions, the nutrient supplies by vertical mixing, and the standing stocks within the mixed layer (following Jouandet et al., 2008) indicated a Si/N export ratio of 3 at A3 versus 4 at C11. In addition, measurements of particulate BSi/PON ratios for sinking particles collected at 200 m depth at station A3 on two occasions ranged from 10 to 73 (Trull et al., 2008, personal communication), confirming strong decoupling during

export. Comparison of our BSi results to PON results obtained by a high-volume pump (Trull et al., 2008) indicates BSi/PON ratios in the standing stock during KEOPS observations from 3 to 59 and thus that this decoupling begins within the mixed layer. Although showing different $\rho Si{:}\rho NO_3$ ratios, both Fe-enriched and HNLC Fe-limited regions behave as "silicate pumps" (Dugdale et al., 1995) (i.e. the differential silicon to nitrogen export from the photic zone) but based upon different mechanisms and with contrasted intensities. In the HNLC area the silica pump appeared as mainly driven by a strong silification of diatoms whereas under a natural Fe-fertilization regime the silica pump was mainly driven by the differential remineralization of N and Si.

Our findings are important because it has been previously hypothesized that changes in $\rho Si{:}\rho NO_3$ uptake ratios (Franck et al., 2005) and the differential export of biogenic silica as compared to particulate organic nitrogen (Dugdale and Wilkerson, 1998) in Fe-limited regions could be responsible for the high-NO_3^-–low-$Si(OH)_4$ conditions prevailing in such areas. Under such assumptions we could expect that Fe availability increases would prevent such decoupling of $Si(OH)_4$ and NO_3^-, as suggested from artificial iron-addition experiments. Fe fertilization would then lead to the almost complete use of NO_3^-, as suggested by the "Si leakage hypothesis" for the last glacial period (Brzezinski et al., 2002). Here we show that natural Fe availability increases can reduce the gap but not totally alleviate the decoupling of $Si(OH)_4$ and NO_3^- utilization, nor the differential silicon to nitrogen export. Our data especially point out that in a natural continously iron-fertilized system, even if the $\rho Si{:}\rho NO_3$ uptake ratio is close to 1, nitrate is not depleted before silicic acid mainly because diatom growth can be supported largely by NH_4^+ recycling. Such major ammonium uptake was generally not detected from artificial mesoscale iron fertilizations (e.g., Frew et al., 2001) probably due to the short duration of the experiments that did not allow the complete establishment of the heterotrophic community (e.g., Zeldis, 2001). From the diatom-dominated south patch of the SOFeX experiment, Coale et al. (2004) reported an *f*-ratio of 0.5–0.6 at day 16 of the experiment suggesting that some regenerated nitrogen was used by the phytoplankton. As observed during KEOPS, against this background of an important role for ammonium recycling, there was an Fe-induced increase in nitrate use, from an initial value of 0.1–0.2.

The NH_4^+ preferential uptake to the detriment of NO_3^- in the KEOPS system suggests that long-term iron fertilization in the Southern Ocean and its subsequent mature ecosystem composed of a diatom bloom regime and an active heterotrophic community would be unlikely to exhaust a major nutrient such as NO_3^- before $Si(OH)_4$.

4.4. Implications for the carbon biological pump functioning

When primarily considering the contribution of an ecosystem to the carbon biological pump, it is important to consider the quantity of C that is exported to depth, which is defined as the intensity of the carbon biological pump (Sarmiento et al., 2004). It follows that one has to estimate the carbon and associated biogenic elements that can leave the system on a definitive basis. This leads us to consider, at least for the particulate biogenic matter, the export fluxes below the depth of the winter mixed layer.

From ^{234}Th analysis, carbon export at 200 m from station A3 ($24.5\,mmol\,m^{-2}\,d^{-1}$) was estimated as twice the level observed at 200 m from C11 (Savoye et al., 2008). In comparison to artificial Fe-fertilization experiments in the Southern Ocean, C export from the natural A3 system is 2–4 times greater (Nodder et al., 2001; Buesseler et al., 2005).

The silicon to carbon uptake and standing stocks ratios can help in understanding the coupling of these two elements in the two contrasted systems from the first step of uptake to the final composition of the biogenic material that could be ultimately exported. At C11 the surface uptake is strongly higher in Si relative to C with the ratio exceeding the ratio of Brzezinski (1985) by a factor of 3 (respectively, 0.39 versus 0.13). In contrast, at A3, the uptake does not show any enrichment in Si relative to C ($\Sigma\rho Si{:}\Sigma\rho C = 0.10 \pm 0.04$ on average). Data of silicon to carbon ratios in the particulate matter that has accumulated in the surface show also a clear contrast between the two systems with the Si:C decoupling less pronounced in the bloom area ($\Sigma Si{:}\Sigma C = 0.23 \pm 0.04$ at A3 versus $\Sigma Si{:}\Sigma C = 0.34 \pm 0.05$ at C11). Thus, if both systems are "silicate pumps" with a decoupling of Si and N cycles, this does not preclude the occurrence of an intense carbon pump at the bloom station as mirrored by a relatively consistent estimated POC export flux.

However, Eppley and Peterson (1979) found that in steady-state conditions, the quantity of carbon exported from a system is numerically equal to mainly NO_3^--based new production. Thus at first sight, a system that does not extensively use NO_3^- as nitrogen source, such as the KEOPS system, would not export large quantities of C. Our findings underline the importance of considering the phytoplankton community structure as well as its nutritional status to derive some conclusions about the fate of biogenic matter. The predominance of regenerated production and the low utilization of NO_3^- as deduced from the study of the nitrogen cycle would suggest a small amount of export *sensu* Eppley and Peterson (1979), while the dominance of large-diatom cells taking up Si and C in balanced proportions would on the contrary suggest a large export. Jacques (1991) already suggested the use of NO_3^--based new production to deduce the C export pattern was not valid for the Southern Ocean accounting for the high unused stocks of NO_3^-. In addition, Eppley and Peterson's concept (1979)-based traditional approach of relying C export to NO_3^--based production is valid only if we consider NO_3^- as the sole nitrogen source supplied to the system from below. In the KEOPS Fe-enriched system, high NH_4^+ stocks persist at depths between 100 and 200 m

(Fig. 2E) in such a way that, due to the high vertical diffusivity coefficient K_Z (Park et al., 2008), NH_4^+ could be supplied in combination with NO_3^- to surface waters to support the almost balanced $NO_3^- - NH_4^+$-based biological production (average *f*-ratio = 0.4 for the four visits at A3). This implies that a part of NH_4^+ utilization could be considered as a new nitrogen source and thus support export production. Plattner et al. (2005) reported from the coastal upwelling system of California that upwelled NH_4^+ contributed to new production although this source was relatively small. Nitrification within the mixed layer is another way in which the link between new production and export can be broken, and there is growing evidence that this does occur, both in the Southern Ocean (Bianchi et al., 1997) and elsewhere in the global ocean (Yool et al., 2007). It is possible that the large-diatom-dominated KEOPS system could be characterized by a decoupling between the C and N cycles as well as between the Si and N cycles, with nitrogen more rapidly recycled than both silica and carbon. The hypothesis of a C/N decoupling in the upper 200 m is compatible with the relatively high amount of exported carbon in spite of low NO_3^- utilization.

A distinction can be made between the intensity of the biological carbon pump (i.e. the quantity of C that is exported to depth) and its efficiency (a measure of its ability to run optimally or not). For this latter, different approaches are used in the literature depending on the timescale considered. Buesseler (1998) used the Thorium-based *e*-ratio, i.e. the ^{234}Th-derived carbon export relative to primary production to assess the short-term efficiency of the pump. Savoye et al. (2008) found that the Th-based *e*-ratio in the fertilized area (13–48% at A3) was lower than in the HNLC area (58% at C11). On the timescale of the entire productive season, the efficiency of the biological pump can be defined as the ability of the system to deplete the macronutrient stocks. Sarmiento et al. (2004) suggest measuring the effectiveness in reducing surface relative to subsurface NO_3^- values. Following this logic, the carbon biological pump in this naturally iron-fertilized system, although stronger than in adjacent HNLC waters (25% at station A3 as compared to 13% at station C11) remains relatively inefficient. This very low efficiency of the carbon biological pump in this naturally iron-fertilized system is also noticeable in the minimal depletion of phosphate (Fig. 2D).

5. Conclusion

During austral summer 2005, the naturally iron-fertilized Kerguelen Plateau was mainly investigated from the study of a reference station that was characterized by a massive diatom bloom persisting in low $Si(OH)_4$ waters ($<2\,\mu M$) gaining by a continuous nutrient vertical supply. Despite high biogenic silica concentrations (average $1101.5 \pm 597.3\,mmol\,m^{-2}$ at A3) silicic acid uptake rates were relatively low (average $7.9 \pm 3.7\,mmol\,m^{-2}\,d^{-1}$) because the diatom bloom was starting to decay. However, the results of Si uptake kinetic experiments also suggest that diatoms of this iron-enriched area were able to grow under low concentrations of silicic acid due to higher affinities for $Si(OH)_4$ in comparison to diatoms from the HNLC off-plateau area, which were more severely Si-limited.

In the iron-enriched area there was a strong decoupling between the seasonal utilization of $Si(OH)_4$ and NO_3^-. We were able to demonstrate that large diatoms rely on the preferential utilization of NH_4^+ and suggest that long-term iron fertilization of the Southern Ocean would not drive the complete depletion of NO_3^- before $Si(OH)_4$ exhaustion. This NH_4^+-based large-diatom development also supports the idea that the Si and C cycles would be decoupled from the N cycle due to differential recycling processes.

The investigation of the Si cycle in the KEOPS area indicates that the siliceous phytoplankton biomass and production are not widely different between the iron-fertilized and the surrounding HNLC waters. Considering the large differences in the two contrasting environments, the moderate differences could be due to two combined effects: (1) the presence of an already decaying diatom bloom over the plateau and (2) the presence of heavily silicified diatoms such as *Fragilariopsis kerguelensis* in HNLC waters.

Acknowledgements

We thank Stephane Blain for taking responsibility for the KEOPS program, and for his assistance through fruitful discussions during all the processing of the presented data. We thank Nicole Garcia, Patrick Raimbault and Valérie Sandroni for providing nutrients, carbon and nitrogen uptake rate data and Hervé Claustre, Joséphine Ras and Julia Uitz for providing pigment data. We also thank Dave Hutchins for his comments on this paper. Finally, we thank the captain Heinrich and his crew of the *Navire Océanographique Marion Dufresne* for allowing us to achieve the cruise in good conditions. This work was supported by the French Research program of INSU-CNRS PROOF (*PROcessus biogéochimiques dans l'Océan et Flux*) and the French Polar Institute IPEV (*Institut Polaire Emile Victor*). L.A. is funded by a European Union *FTP6 Marie Curie* International Incoming Fellowship. The manuscript was improved from comments of two anonymous reviewers.

References

Aksnes, D.L., Egge, J.K., 1991. A theoretical model for nutrient uptake in phytoplankton. Marine Ecology Progress Series 70, 65–72.

Armand, L., Cornet-Barthau, V., Mosseri, J., Quéguiner, B., 2008. Late summer diatom biomass and community structure on and around the naturally iron-fertilized Kerguelen plateau in the Southern Ocean. Deep-Sea Research II, this issue [doi:10.1016/j.dsr2.2007.12.031].

Bianchi, M., Feliatra, F., Treguer, P., Vincendeau, M.A., Morvan, J., 1997. Nitrification rates, ammonium and nitrate distribution in upper layers of the water column and in sediments of the Indian sector of the Southern Ocean. Deep-Sea Research I 44 (5), 1017–1032.

Blain, S., Quéguiner, B., Armand, L., Belviso, S., Bombled, B., Bopp, L., Bowie, A., Brunet, C., Brussaard, C., Carlotti, F., Cristaki, U.,

Corbière, A., Durand, I., Ebersbach, F., Fuda, J.-L., Garcia, N., Gerringa, L., Griffiths, B., Guigue, C., Guillerm, C., Jacquet, S., Jeandel, C., Laan, P., Lefèvre, D., Lomonaco, C., Malits, A., Mosseri, J., Obernosterer, I., Park, Y.-H., Picheral, M., Pondaven, P., Remenyi, T., Sandroni, V., Sarthou, G., Savoye, N., Scouarnec, L., Souhaut, M., Thuiller, D., Timmermans, K., Trull, T., Uitz, J., van-Beek, P., Veldhuis, M., Vincent, D., Viollier, E., Vong, L., Wagener, T., 2007. Impacts of natural iron fertilisation on the Southern Ocean. Nature 446, 1070–1074.

Blain, S., Sarthou, G., Laan, P., 2008. Distribution of dissolved iron during the natural iron fertilization experiment KEOPS (Kerguelen Plateau, Southern Ocean). Deep-Sea Research II, this issue [doi:10.1016/j.dsr2.2007.12.028].

Boyd, P.W., Muggli, D.L., Varela, D.E., Goldblatt, R.H., Chretien, R., Orians, K.J., Harrison, P.J., 1996. *In vitro* iron enrichment experiments in the NE subarctic Pacific. Marine Ecology Progress Series 136, 179–193.

Boyd, P., LaRoche, J., Gall, M., Frew, R., McKay, R.M.L., 1999. Role of iron, light, and silicate in controlling algal biomass in subantarctic waters SE of New Zealand. Journal of Geophysical Research 104 (C6), 13,395–13,408.

Boyd, P.W., Watson, A.J., Law, C.S., Abraham, E.R., Trull, T., Murdoch, R., Bakker, D.C.E., Bowie, A.R., Buesseler, K.O., Chang, H., Charette, M., Croot, P., Downing, K., Frew, R., Gall, M., Hadfield, M., Hall, J., Harvey, M., Jameson, G., LaRoche, J., Liddicoat, M., Ling, R., Maldonado, M.T., McKay, R.M., Nodder, S., Pickmere, S., Pridmore, R., Rintoul, S., Safi, K., Sutton, P., Strzepek, R., Tanneberger, K., Turner, S., Waite, A., Zeldis, J., 2000. A mesoscale phytoplankton bloom in the polar Southern Ocean stimulated by iron fertilization. Nature 407, 695–702.

Boyd, P.W., Law, C.S., Wong, C.S., Nojiri, Y., Tsuda, A., Levasseur, M., Takeda, S., Rivkin, R., Harrison, P.J., Strzepek, R., Gower, J., McKay, R.M., Abraham, E., Arychuk, M., Barwell-Clarke, J., Crawford, W., Hale, M., Harada, K., Johnson, K., Kiyosawa, H., Kudo, I., Marchetti, A., Miller, W., Needoba, J., Nishioka, J., Ogawa, H., Page, J., Robert, M., Saito, H., Sastri, A., Sherry, N., Soutar, T., Sutherland, N., Taira, Y., Whitney, F., Emmy Wong, S.K., Yoshimura, T., 2004. The decline and fate of an iron induced subarctic phytoplankton bloom. Nature 428, 549–553.

Boyd, P.W., Strzepek, R., Takeda, S., Jackson, G., Wong, C.S., McKay, R.M., Law, C., Kiyosawa, H., Saito, H., Nelson, S., Johnson, K., Gower, J., Ramaiah, N., 2005. The evolution and termination of an iron-induced mesoscale bloom in the northeast subarctic Pacific. Limnology and Oceanography 50 (6), 1872–1886.

Brooks, S.P.G., 1992. A simple computer program with statistical tests for the analysis of enzyme kinetics. Biotechniques 13, 906–911.

Brown, L., Sanders, R., Savidge, G., Lucas, C.H., 2003. The uptake of silica during the spring bloom in the Northeast Atlantic Ocean. Limnology and Oceanography 48 (5), 1831–1845.

Brzezinski, M.A., 1985. The Si:C:N ratio of marine diatoms: interspecific variability and the effect of some environmental variables. Journal of Phycology 21, 347–357.

Brzezinski, M.A., Nelson, D.M., 1989. Seasonal changes in the silicon cycle within a Gulf Stream warm-core ring. Deep-Sea Research I 36 (7), 1009–1030.

Brzezinski, M.A., Nelson, D.M., 1995. The annual silica cycle in the Sargasso Sea near Bermuda. Deep-Sea Research I 42, 1215–1237.

Brzezinski, M.A., Nelson, D.M., 1996. Chronic substrate limitation of silicic acid uptake rates in the western Sargasso Sea. Deep-Sea Research II 43 (2–3), 437–453.

Brzezinski, M.A., Villareal, T.A., Lipschultz, F., 1998. Silica production and the contribution of diatoms to new and primary production in the central North Pacific. Marine Ecology Progress Series 167, 89–104.

Brzezinski, M.A., Nelson, D.M., Franck, V.M., Sigmon, D.E., 2001. Silicon dynamics within an intense open-ocean diatom bloom in the Pacific sector of the Southern Ocean. Deep-Sea Research II 48, 3997–4018.

Brzezinski, M.A., Pride, C.J., Franck, V.M., Sigman, D.M., Sarmiento, J.L., Matsumoto, K., Gruber, N., Rau, G.H., Coale, K.H., 2002. A switch from $Si(OH)_4$ to NO_3^- depletion in the glacial Southern Ocean. Geophysical Research Letters 29 (12).

Brzezinski, M.A., Dickson, M.L., Nelson, D.M., Sambrotto, R., 2003. Ratios of Si, C and N uptake by microplankton in the Southern Ocean. Deep-Sea Research II 50, 619–633.

Brzezinski, M.A., Jones, J.L., Demarest, M., 2005. Control of silica production by iron and silicic acid during the Southern Ocean Iron Experiment (SOFeX). Limnology and Oceanography 50 (3), 810–824.

Buesseler, K.O., 1998. The decoupling of production and particulate export in the surface ocean. Global Biogeochemical Cycles 12, 297–310.

Buesseler, K.O., Andrews, J.E., Pike, S.M., Charette, M.A., Goldson, L.E., Brzezinski, M.A., Lance, V.P., 2005. Particle export during the Southern Ocean Iron Experiment (SOFeX). Limnology and Oceanography 50 (1), 311–327.

Carlotti, F., Thibault-Botha, D., Nowaczyk, A., Lefèvre, D., 2008. Zooplankton community structure, biomass and role in carbon fluxes during the second half of a phytoplankton bloom in the eastern sector of the Kerguelen shelf (January–February 2005). Deep Sea Research II, this issue [doi:10.1016/j.dsr2.2007.12.010].

Charette, M.A., Buesseler, K.O., 2000. Does iron fertilization lead to rapid carbon export in the Southern Ocean? Geochemistry Geophysics Geosystems 1, Paper no. 2000GC000069.

Claquin, P., Martin-Jézéquel, V., Kromkamp, J.C., Veldhuis, M.J.W., Kraay, G.W., 2002. Uncoupling of silicon compared with carbon and nitrogen metabolisms and the role of the cell cycle in continuous cultures of *Thalassiosira pseudonana* (Bacillariophyceae) under light, nitrogen, and phosphorus control. Journal of Phycology 38, 922–930.

Coale, K.H., Johnson, K.S., Fitzwater, S.E., Gordon, R.M., Tanner, S., Chavez, F.P., Ferioli, L., Sakamoto, C., Rogers, P., Millero, F., Steinberg, P., Nightingale, P., Cooper, D., Cochlan, W.P., Landry, M.R., Constantinou, J., Rollwagen, G., Trasvina, A., Kudela, R., 1996. A massive phytoplankton bloom induced by an ecosystem-scale iron fertilization experiment in the equatorial Pacific Ocean. Nature 383, 495–501.

Coale, K.H., Johnson, K.S., Chavez, F.P., Buesseler, K.O., Barber, R.T., Brzezinski, M.A., Cochlan, W.P., Millero, F.J., Falkowski, P.G., Bauer, J.E., Wanninkhof, R.H., Kudela, R.M., Altabet, M.A., Hales, B.E., Takahashi, T., Landry, M.R., Bidigare, R.R., Wang, X., Chase, Z., Strutton, P.G., Friederich, G.E., Gorbunov, M.Y., Lance, V.P., Hilting, A.K., Hiscock, M.R., Demarest, M., Hiscock, W.T., Sullivan, K.F., Tanner, S.J., Mike Gordon, R., Hunter, C.N., Elrod, V.A., Fitzwater, S.E., Jones, J.L., Tozzi, S., Koblizek, M., Roberts, A.E., Herndon, J., Brewster, J., Ladizinsky, N., Smith, G., Cooper, D., Timothy, D., Brown, S.L., Selph, K.E., Sheridan, C.C., Twining, B.S., Johnson, Z.I., 2004. Southern Ocean iron enrichment experiment: carbon cycling in high- and low-Si waters. Science 304, 408–414.

Cornet-Barthaux, V., Armand, L.K., Quéguiner, B., 2007. Biovolume and biomass measurements on key Southern Ocean diatoms. Aquatic Microbial Ecosystems 48, 295–308.

Cullen, J.J., 1991. Hypotheses to explain high-nutrient conditions in the open sea. Limnology and Oceanography 36, 1578–1599.

De Baar, H.J.W., Boyd, P.W., Coale, K.H., Landry, M.R., Tsuda, A., Assmy, P., Bakker, D.C.E., Bozec, Y., Barber, R.T., Brzezinski, M.A., Buesseler, K.O., Boyé, M., Croot, P.L., Gervais, F., Gorbunov, M.Y., Harrison, P.J., Hiscock, W.T., Laan, P., Lancelot, C., Law, C.S., Levasseur, M., Marchetti, A., Millero, F.J., Nishioka, J., Nojiri, Y., van Oijen, T., Riesebell, U., Rijkenberg, M.J.A., Saito, H., Takeda, S., Timmermans, K.R., Veldhuis, M.J.W., Waite, A.M., Wong, C.S., 2005. Synthesis of iron fertilization experiments: from the iron age in the age of enlightenment. Journal of Geophysical Research 110, C09S16.

De La Rocha, C.L., Hutchins, D.A., Brzezinski, M.A., Zhang, Y., 2000. Effects of iron and zinc deficiency on elemental composition and silica production by diatoms. Marine Ecology Progress Series 195, 71–79.

Dortch, Q., 1990. The interaction between ammonium and nitrate uptake in phytoplankton. Marine Ecology Progress Series 61, 183–201.

Dugdale, R.C., Wilkerson, F.P., 1998. Silicate regulation of new production in the equatorial Pacific upwelling. Nature 391, 270–273.

Dugdale, R.C., Wilkerson, F.P., Minas, H.J., 1995. The role of a silicate pump in driving new production. Deep-Sea Research I 5 (42), 697–719.

Egge, J.K., Aksnes, D.L., 1992. Silicate as regulating nutrient in phytoplankton competition. Marine Ecology Progress Series 83, 281–289.

Eppley, R.W., Peterson, B.J., 1979. Particulate organic matter flux and planktonic new production in the deep ocean. Nature 282, 677–680.

Franck, V.M., Brzezinski, M.A., Coale, K.H., Nelson, D.M., 2000. Iron and silicic acid concentrations regulate Si uptake north and south of the Polar Frontal Zone in the Pacific Sector of the Southern Ocean. Deep-Sea Research II 47, 3315–3338.

Franck, V.M., Smith, G.J., Bruland, K.W., Brzezinski, M.A., 2005. Comparison of size-dependent carbon, nitrate, and silicic acid uptake rates in high- and low-iron waters. Limnology and Oceanography 50 (3), 825–838.

Frew, R., Bowie, A., Croot, P., Pickmere, S., 2001. Macronutrient and trace-metal geochemistry of an *in situ* iron-induced Southern Ocean bloom. Deep Sea Research II 48 (11–12), 2467–2481.

Gerringa, L.J.A., Blain, S., Laan, P., Sarthou, G., Veldhuis, M.J.W., Brussaard, C.P.D., Viollier, E., Timmermans, K.R., 2008. Fe- binding dissolved organic ligands near the Kerguelen archipelago in the Southern Ocean (Indian sector). Deep-Sea Research II, this issue [doi:10.1016/j.dsr2.2007.12.007].

Healey, F.P., 1980. Slope of the Monod equation as an indicator of advantage in nutrient competition. Microbial Ecology 5, 281–286.

Holmes, R.M., Aminot, A., Kerouel, R., Hooker, B.A., Peterson, B.J., 1999. A simple and precise method for measuring ammonium in marine and freshwater ecosystems. Canadian Journal of Fisheries and Aquatic Sciences 56, 1801–1808.

Hutchins, D.A., Bruland, K.W., 1998. Iron-limited diatom growth and Si:N uptake ratios in a coastal upwelling regime. Nature 393, 561–564.

Hutchins, D.A., DiTullio, G.R., Zhang, Y., Bruland, K.W., 1998. An iron limitation mosaic in the California upwelling regime. Limnology and Oceanography 43 (6), 1037–1054.

Hutchins, D.A., Franck, V.M., Brzezinski, M.A., Bruland, K.W., 1999. Inducing phytoplankton iron limitation in iron-replete coastal waters with a strong chelating ligand. Limnology and Oceanography 44 (4), 1009–1018.

Hutchins, D.A., Sedwick, P.N., DiTullio, G.R., Boyd, P.W., Quéguiner, B., Griffiths, F.B., Crossley, C., 2001. Control of phytoplankton growth by iron and silicic acid availability in the subantarctic Southern Ocean: experimental results from the SAZ Project. Journal of Geophysical Research 106 (C12), 31,559–31,572.

Jacques, G., 1991. Is the concept of new production-regenerated production valid for the Southern Ocean? Marine Chemistry 35, 273–286.

Jeffrey, S.W., Mantoura, R.F.C., Wright, S.W., 1997. Phytoplankton Pigments in Oceanography: Guidelines to Modern Methods. Monographs on Oceanographic Methodology, vol. 10. UNESCO Publishing, Paris, France, 662pp.

Jouandet, M.P., Blain, S., Metzl, N., Brunet, C., Trull, T., Obernosterer, I., 2008. A seasonal carbon budget for a naturally iron-fertilized bloom over the Kerguelen Plateau in the Southern Ocean. Deep-Sea Research II, this issue [doi:10.1016/j.dsr2.2007.12.037].

Kumar, N., Anderson, R.F., Mortlock, R.A., Froelich, P.N., Kubik, P., Dittrich-Hannen, B., Suter, M., 1995. Increased biological productivity and export production in the glacial Southern Ocean. Nature 378, 675–680.

Leblanc, K., Leynaert, A., Fernandez, I.C., Rimmelin, P., Moutin, T., Raimbault, P., Ras, J., Quéguiner, B., 2005. A seasonal study of diatom dynamics in the North Atlantic during the POMME experiment (2001): evidence for Si limitation of the spring bloom. Journal of Geophysical Research 110, C07S14.

Leynaert, A., 1993. La production de la Silice Biogénique dans l'Ocean: de la Mer de Weddell a l'Ocean Antarctique. Ph.D. Thesis, Université Pierre et Marie Curie, Paris, France, 100pp.

Leynaert, A., Bucciarelli, E., Claquin, P., Dugdale, R.C., Martin-Jézéquel, V., Pondaven, P., Ragueneau, O., 2004. Effect of iron deficiency on diatom cell size and silicic acid uptake kinetics. Limnology and Oceanography 49 (4), 1134–1143.

Martin, J.H., 1990. Glacial–Interglacial CO_2 change: the iron hypothesis. Paleoceanography 5 (1), 1–13.

Martin-Jézéquel, V., Hildebrand, M., Brzezinski, M.A., 2000. Silicon metabolism in diatoms: implications for growth. Journal of Phycology 36, 821–840.

Minas, H.J., Minas, M., Packard, T.T., 1986. Productivity in upwelling areas deduced from hydrographic and chemical fields. Limnology and Oceanography 31, 1182–1206.

Morel, F.M.M., Rueter, J.G., Price, N.M., 1991. Iron nutrition of phytoplankton and its possible importance in the ecology of ocean regions with high nutrient and low biomass. Oceanography 4, 56–60.

Nelson, D.M., Dortch, Q., 1996. Silicic acid depletion and silicon limitation in the plume of the Mississippi River: evidence from kinetic studies in spring and summer. Marine Ecology Progress Series 136, 163–178.

Nelson, D.M., Goering, J.J., 1978. Assimilation of silicic acid by phytoplankton in the Baja California and northwest Africa upwelling systems. Limnology and Oceanography 23 (3), 508–517.

Nelson, D.M., Tréguer, P., 1992. Role of silicon as a limiting nutrient to Antarctic diatoms: evidence from kinetic studies in the Ross Sea ice-edge zone. Marine Ecology Progress Series 80, 255–264.

Nelson, D.M., Brzezinski, M.A., Sigmon, D.E., Franck, V.M., 2001. A seasonal progression of Si limitation in the Pacific sector of the Southern Ocean. Deep-Sea Research II 48, 3973–3995.

Nodder, S.D., Charette, M.A., Waite, A.M., Trull, T.W., Boyd, P.W., Zeldis, J., Buesseler, K.O., 2001. Particle transformations and export flux during an *in situ* iron-stimulated bloom in the Southern Ocean. Geophysical Research Letters 28 (12), 2409–2412.

Obernosterer, I., Christaki, U., Lefèvre, D., Catala, P., Van Wambeke, F., Le Baron, P., 2008. Rapid bacterial mineralization of organic carbon produced during a phytoplankton bloom induced by natural iron fertilization in the Southern Ocean. Deep-Sea Research II, this issue [doi:10.1016/j.dsr2.2007.12.005].

Park, Y.H., Fuda, J.L., Durand, I., Naveira Garabato, A.C., 2008. Internal tides and vertical mixing over the Kerguelen Plateau. Deep-Sea Research II, this issue [doi:10.1016/j.dsr2.2007.12.027].

Plattner, G.K., Gruber, N., Frenzel, H., McWilliams, J.C., 2005. Decoupling marine export production from new production. Geophysical Research Letters 32, L11612.

Pondaven, P., Ruiz-Pino, D., Fravalo, C., Tréguer, P., Jeandel, C., 2000. Interannual variability of Si and N cycles at the time-series station KERFIX between 1990 and 1995—a 1-D modelling study. Deep-Sea Research I 47, 223–257.

Quéguiner, B., 2001. Biogenic silica production in the Australian sector of the Subantarctic Zone of the Southern Ocean in late summer 1998. Journal of Geophysical Research 106 (C12), 31,627–31,636.

Quéguiner, B., Brzezinski, M.A., 2002. Biogenic silica production rates and particulate organic matter distribution in the Atlantic sector of the Southern Ocean during austral spring 1992. Deep-Sea Research II 49, 1765–1786.

Quéguiner, B., Tréguer, P., Peeken, I., Scharek, R., 1997. Biogeochemical dynamics and the silicon cycle in the Atlantic sector of the Southern Ocean during austral spring 1992. Deep-Sea Research II 44 (1–2), 69–89.

Ragueneau, O., Tréguer, P., Leynaert, A., Anderson, R.F., Brzezinski, M.A., DeMaster, D.J., Dugdale, R.C., Dymond, J., Fischer, G., Franç ois, R., Heinze, C., Maier-Reimer, E., Martin-Jézéquel, V., Nelson, D.M., Quéguiner, B., 2000. A review of the Si cycle in the modern ocean: recent progress and missing gaps in the application of biogenic opal as a paleoproductivity proxy. Global and Planetary Change 26, 317–365.

Ragueneau, O., Savoye, N., Del Amo, Y., Cotten, J., Tardiveau, B., Leynaert, A., 2005. A new method for the measurement of biogenic silica in suspended matter of coastal waters: using Si:Al ratios to correct for the mineral interference. Continental Shelf Research 25, 697–710.

Raimbault, P., Diaz, F., Pouvesle, W., Boudjellal, B., 1999. simultaneous determination of particulate forms of carbon, nitrogen and phosphorus collected on filters using a semi-automatic wet-oxidation procedure. Marine Ecology Progress Series 180, 289–295.

Sarmiento, J.L., Dunne, J., Armstrong, R.A., 2004. Do we now understand the Ocean's biological pump? US JGOFS News 12 (4), 1–5.

Sarthou, G., Timmermans, K.R., Blain, S., Tréguer, P., 2005. Growth physiology and fate of diatoms in the ocean: a review. Journal of Sea Research 53, 25–42.

Sarthou, G., Vincent, D., Christaki, U., Obernosterer, I., Timmermans, K.R., Brussaard, C.P.D., 2008. The fate of biogenic iron during a phytoplankton bloom induced by natural fertilization: impact of copepod grazing. Deep-Sea Research II, this issue [doi:10.1016/j.dsr2.2007.12.033].

Savoye, N., Trull, T.W., Jacquet, S.H.M., Navez, J., Dehairs, F., 2008. ^{234}Th-based export fluxes during a natural iron fertilization experiment in the Southern Ocean (KEOPS). Deep-Sea Research II, this issue [doi:10.1016/j.dsr2.2007.12.036].

Sedwick, P.N., Blain, S., Quéguiner, B., Griffiths, F.B., Fiala, M., Bucciarelli, E., Denis, M., 2002. Resource limitation of phytoplankton growth in the Crozet Basin, Subantarctic Southern Ocean. Deep-Sea Research II 49, 3327–3349.

Sigman, D.M., Boyle, E.A., 2000. Glacial/Interglacial variations in atmospheric carbon dioxide. Nature 407, 859–869.

Smetacek, V., Assmy, P., Henjes, J., 2004. The role of grazing in structuring Southern Ocean pelagic ecosystems and biogeochemical cycles. Antarctic Science 16 (4), 541–558.

Smith, W.O., Nelson, D.M., 1986. Importance of ice edge phytoplankton production in the Southern Ocean. BioSciences 36 (4), 251–257.

Takeda, S., 1998. Influence of iron availability on nutrient consumption ratio of diatoms in oceanic waters. Nature 393, 774–777.

Thompson, P.A., Levasseur, M.E., Harrisson, P.J., 1989. Light-limited growth on ammonium vs. Nitrate: What is the advantage for marine phytoplankton? Limnology and Oceanography 34 (6), 1014–1024.

Trull, T.W., Rintoul, S.R., Hadfield, M., Abraham, E.R., 2001. Circulation and seasonal evolution of Polar waters south of Australia: implications for iron fertilisation of the Southern Ocean. Deep-Sea Research II 48 (11/12), 2439–2466.

Trull, T., Davies, D., Casciotti, K., 2008. Insights into nutrient assimilation and export in naturally iron-fertilized waters of the Southern Ocean from nitrogen, carbon and oxygen isotopes. Deep-Sea Research II, this issue [doi:10.1016/j.dsr2.2007.12.035].

Tréguer, P., Le Corre, P., 1975. Manuel d'Analyse des Sels Nutritifs dans l'Eau de Mer. Utilisation de l'Auto Analyser II Technicon. Laboratoire d'Océanographie Chimique, U.B.O., Brest, France.

Uitz, J., Claustre, H., Griffiths, B., Ras, J., in preparation. A phytoplankton class-specific primary production model applied to the Kerguelen Islands region (Southern Ocean).

Van Heukelem, L., Thomas, C.S., 2001. Computer-assisted high-performance liquid chromatography method development with applications to the isolation and analysis of phytoplankton pigments. Journal of Chromatography A 910 (1), 31–49.

Wheeler, P.A., Kokkinakis, S.A., 1990. Ammonium recycling limits nitrate use in the oceanic subarctic Pacific. Limnology and Oceanography 35 (6), 1267–1278.

Yool, A., Martin, A.P., Fernandez, C., Clarck, D.R., 2007. The significance of nitrification for oceanic new production. Nature 447, 999–1002.

Zeldis, J., 2001. Mesozooplankton community composition, feeding, and export production during SOIREE. Deep-Sea Research II 48 (11–12), 2615–2634.